

# A Chronic Increase in Blood-Brain Barrier Permeability Facilitates Intraneuronal Deposition of Exogenous Bloodborne Amyloid-Beta<sub>1–42</sub> Peptide in the Brain and Leads to Alzheimer's Disease-Relevant Cognitive Changes in a Mouse Model

Nimish K. Acharya<sup>a,b,c,d,e,f,1</sup>, Henry C. Grossman<sup>g,1</sup>, Peter M. Clifford<sup>a,h</sup>, Eli C. Levin<sup>a,i</sup>, Kenneth R. Light<sup>j</sup>, Hana Choi<sup>e</sup>, Randel L. Swanson II<sup>c,k,1</sup>, Mary C. Kosciuk<sup>a</sup>, Venkat Venkataraman<sup>b,m</sup>, David J. Libon<sup>a,n</sup>, Louis D. Matzel<sup>g</sup> and Robert G. Nagele<sup>a,d,e,f,\*</sup>

<sup>a</sup>*Department of Geriatrics and Gerontology, New Jersey Institute for Successful Aging, Rowan-Virtua School of Osteopathic Medicine, Rowan University, Stratford, NJ, USA*

<sup>b</sup>*Department of Cell Biology and Neuroscience, Rowan-Virtua School of Osteopathic Medicine, Rowan University, Stratford, NJ, USA*

<sup>c</sup>*Center for Neurotrauma, Neurodegeneration and Restoration, Corporal Michael J. Crescenzo VA Medical Center, Philadelphia, PA, USA*

<sup>d</sup>*Biomarker Discovery Center, New Jersey Institute for Successful Aging (NJISA), Rowan-Virtua School of Osteopathic Medicine, Stratford, NJ, USA*

<sup>e</sup>*Rowan-Virtua Graduate School of Biomedical Sciences, Stratford, NJ, USA*

<sup>f</sup>*Rowan-Virtua School of Translational Biomedical Engineering and Sciences, Rowan University, Glassboro, NJ, USA*

<sup>g</sup>*Department of Psychology, Rutgers University, Piscataway, NJ, USA*

<sup>h</sup>*HNL Lab Medicine, Allentown, PA, USA*

<sup>i</sup>*Department of Graduate Medical Education, Bayhealth Medical Center, Dover, DE, USA*

<sup>j</sup>*Department of Psychology, Barnard College of Columbia University, New York, NY, USA*

<sup>k</sup>*Rehab Medicine Service, Corporal Michael J. Crescenzo VA Medical Center, Philadelphia, PA, USA*

<sup>l</sup>*Department of Physical Medicine and Rehabilitation, University of Pennsylvania Perelman School of Medicine, Philadelphia, PA, USA*

<sup>m</sup>*Department of Academic and Student Affairs, Rowan-Virtua School of Osteopathic Medicine, Stratford, NJ, USA*

<sup>n</sup>*Department of Psychology, Rowan University, Glassboro, NJ, USA*

Handling Associate Editor: David Loewenstein

Accepted 26 December 2023

Pre-press 20 February 2024

<sup>1</sup>These authors contributed equally to this work.

\*Correspondence to: Dr. Robert G. Nagele, 2 Medical Center Dr., Science Center, Room #313A, Stratford, NJ 08084, USA. Tel.: +856 566 6083; E-mail: nagele@rowan.edu.

**Abstract.**

**Background:** Increased blood-brain barrier (BBB) permeability and amyloid- $\beta$  (A $\beta$ ) peptides (especially A $\beta$ <sub>1–42</sub>) (A $\beta$ <sub>42</sub>) have been linked to Alzheimer's disease (AD) pathogenesis, but the nature of their involvement in AD-related neuropathological changes leading to cognitive changes remains poorly understood.

**Objective:** To test the hypothesis that chronic extravasation of bloodborne A $\beta$ <sub>42</sub> peptide and brain-reactive autoantibodies and their entry into the brain parenchyma via a permeable BBB contribute to AD-related pathological changes and cognitive changes in a mouse model.

**Methods:** The BBB was rendered chronically permeable through repeated injections of *Pertussis* toxin (PT), and soluble monomeric, fluorescein isothiocyanate (FITC)-labeled or unlabeled A $\beta$ <sub>42</sub> was injected into the tail-vein of 10-month-old male CDI mice at designated intervals spanning ~3 months. Acquisition of learned behaviors and long-term retention were assessed via a battery of cognitive and behavioral tests and linked to neuropathological changes.

**Results:** Mice injected with both PT and A $\beta$ <sub>42</sub> demonstrated a preferential deficit in the capacity for long-term retention and an increased susceptibility to interference in selective attention compared to mice exposed to PT or saline only. Immunohistochemical analyses revealed increased BBB permeability and entry of bloodborne A $\beta$ <sub>42</sub> and immunoglobulin G (IgG) into the brain parenchyma, selective neuronal binding of IgG and neuronal accumulation of A $\beta$ <sub>42</sub> in animals injected with both PT and A $\beta$ <sub>42</sub> compared to controls.

**Conclusions:** Results highlight the potential synergistic role of BBB compromise and the influx of bloodborne A $\beta$ <sub>42</sub> into the brain in both the initiation and progression of neuropathologic and cognitive changes associated with AD.

Keywords: A $\beta$ <sub>42</sub>, Alzheimer's disease, amyloid-beta peptides, amyloid plaques, autoantibodies, blood-brain barrier, dementia, immunoglobulin G

## INTRODUCTION

Alzheimer's disease (AD) is a neurodegenerative disorder characterized by progressive destruction and loss of neurons and their synapses in the brain, gradually escalating cognitive decline and, ultimately, dementia and death [1–6]. Currently, treatment options are limited and, at best, only temporarily alleviate some symptoms with no significant effect on disease progression [7–9]. Seeking a better understanding of events and conditions that trigger and propagate AD pathogenesis is critical before effective disease-modifying therapies can be proposed and tested in clinical trials. Despite progress in our understanding of some key aspects of AD-related neuropathological and cognitive deficits, a complete picture of sequential stages during AD pathogenesis and its relationship with neuropsychological phenotypic outcome remains elusive [3, 5]. AD has been associated with a number of pathological features, including reactive gliosis, inflammation, and the appearance of hallmark amyloid plaques (APs) and neurofibrillary tangles (NFTs). These and other changes in the brain have been temporally and spatially linked to a progressive and severe decline in cognitive function [10–12].

To identify potential early triggers of AD, determine its pathogenetic course, and ascertain which pathological features play a central role in driving the observed cognitive, memory and behavioral changes,

much research has focused on APs, NFTs, neuroinflammation, and vascular pathology [13]. While the exact nature and magnitude of the contribution of each of these pathological features to disease progression continue to be debated, there is little doubt that the appearance of APs and NFTs in the brain parenchyma is directly linked to AD pathogenesis. It is generally thought that brain amyloid deposition in the form of APs precedes the appearance of NFTs [14–18]. APs principally contain the amyloid- $\beta$ <sub>1–42</sub> (A $\beta$ <sub>42</sub>) peptide, a self-assembling amyloidogenic peptide composed of 42 amino acid residues derived from cleavage of the amyloid- $\beta$  protein precursor (A $\beta$ PP) [19–25]. Increased production of A $\beta$ <sub>42</sub> and its deposition in the brains of patients with early onset, familial AD, as well as in certain transgenic mice, have confirmed correlations between A $\beta$ <sub>42</sub> levels and the formation of APs, loss of synapses, and cognitive deficits [15, 26–29]. Numerous studies have described A $\beta$ <sub>42</sub> deposition in the form of APs and intraneuronal deposits, the latter primarily in the perikaryon of pyramidal cells in humans, transgenic rodents, and *in vitro* models [15, 25, 30–51]. Mechanisms associated with intraneuronal A $\beta$ <sub>42</sub> deposition at each of these sites and their relationship to neuronal dysfunction and loss are being investigated [52, 53]. Determining the source(s) of the A $\beta$ <sub>42</sub> peptide that eventually deposits within neurons and APs in the brain and the underlying reason for the requirement of advanced age remain key questions.

Aging-associated changes in the structural and functional integrity of blood vessels in the human brain have been extensively studied. Among these changes, a chronic increase in blood-brain barrier (BBB) permeability, resulting in a disruption of brain homeostasis, has long been suspected of playing a role in the triggering and/or progression of AD as well as in other neurodegenerative diseases, post-operative delirium, post-operative cognitive decline, Sundowner's syndrome and the short- and long-term effects of traumatic brain injury [31, 54–64]. There is some evidence that increased BBB permeability allows greater access of bloodborne A $\beta$  peptides to neurons residing in the brain parenchyma [31]. A $\beta$  peptides are detected in human blood and cerebrospinal fluid (CSF) [65–70]. Since A $\beta$ <sub>42</sub> peptide is detected in the blood (plasma) of both cognitively normal and AD subjects, it is not unreasonable to suspect that, in the context of BBB compromise and a prolonged pre-symptomatic phase, the blood could serve as a chronic source of the A $\beta$ <sub>42</sub> peptide that is deposited in AD brains [31, 65–70]. This scenario is supported by our earlier reports demonstrating the extravasation of various vascular components into the brain parenchyma in both AD and age-match nondemented controls [31, 71]. Our previous studies of human, porcine, rat and mouse brain have demonstrated a close spatial association between BBB leak sites and the locations of A $\beta$ <sub>42</sub>-burdened neurons [31, 72, 73]. For example, in a study on mice with an acutely compromised BBB, we tracked the fate of bloodborne, soluble A $\beta$ <sub>42</sub> peptide and demonstrated that it readily entered the brain, was selectively bound to pyramidal neurons and was internalized by these cells, the same neuronal subtype that is typically overburdened with A $\beta$ <sub>42</sub>-rich deposits in human AD brains [31].

In the present study, we used the middle-aged (10 months old) mouse as a model system to investigate the long-term neuropathological effects of a chronically induced increase in BBB permeability and the resulting influx of soluble bloodborne fluorescein isothiocyanate (FITC)-labeled and unlabeled A $\beta$ <sub>42</sub> into the brain parenchyma on the animals' ability to learn (acquisition) and retain (long-term memory) information, as well as on selective attention. To induce chronic BBB dysfunction, *Pertussis* toxin (PT) was repeatedly injected into the tail vein of 10-month-old male CD1 mice for a little over three months. Mice also received tail vein injections of purified monomeric FITC-labeled or unlabeled A $\beta$ <sub>42</sub> peptide at regular intervals over the same

time period. During the last month of treatment, animals underwent a battery of cognitive and behavioral assessments. Mice injected with PT plus A $\beta$ <sub>42</sub> demonstrated a deficit in long-term retention and increased susceptibility to interference in selective attention compared to controls exposed to either PT or saline only. Immunohistochemical analyses of brain samples revealed an increased influx of A $\beta$ <sub>42</sub> and IgG into the brain parenchyma, selective neuronal binding of IgG, and intraneuronal accumulation of exogenous A $\beta$ <sub>42</sub> in mice injected with PT plus A $\beta$ <sub>42</sub> compared to controls. These findings highlight the potential contribution of an impaired BBB and the resulting influx of soluble, bloodborne A $\beta$ <sub>42</sub> into the brain parenchyma in triggering the earliest cognitive and neuropathological changes associated with AD-related pathogenesis.

## MATERIALS AND METHODS

### *Animals*

All procedures involving animals were performed following the guidelines of the institutional animal care and use committee (IACUC) in accordance with NIH guidelines. Ten-month-old male CD-1 mice (Harlan) were randomly separated into three treatment groups: PT-A $\beta$ <sub>42</sub> (n = 20) (animals injected with both PT and A $\beta$ <sub>42</sub>), saline (Sal) only controls (i.e., where PT and A $\beta$ <sub>42</sub> injections were each replaced with saline) (n = 12), and PT-Sal controls (i.e., animals injected with PT but with A $\beta$ <sub>42</sub> injections replaced with saline) (n = 12). Animals were acclimated to the laboratory for 14 days prior to the initiation of any treatments and were handled (held and manipulated by an experimenter) for 90 s/day during this period. This handling ensured that differential stress responses to the experimenters and any associated effects on learning were minimized. Animals were individually housed in clear boxes with floors lined with wood shavings in a humidity- and temperature-controlled vivarium adjacent to testing rooms. A 12/12-h light/dark cycle was maintained.

### *Preparation of A $\beta$ <sub>42</sub> peptides and PT*

A $\beta$  peptides (FITC-A $\beta$ <sub>42</sub>, Anaspec, San Jose, CA; unlabeled A $\beta$  peptides, Biosource, Camarillo, CA) were solubilized to the monomeric form according to the method described by Zagorski et al. (1999) [74]. Briefly, A $\beta$  peptide was solubilized

(1 mg/ml) in trifluoroacetic acid (TFA), followed by removal of TFA under a slow, steady stream of nitrogen gas. This was followed by three sequential solubilizations in 1,1,1,3,3,3-hexafluoroisopropanol (HFIP) followed by removal of HFIP under nitrogen gas each time. Stock solutions (50.0  $\mu$ M) were prepared in 0.5 $\times$ PBS, 250.0 mM HEPES buffer (pH 8.5). Working solutions were diluted in 0.9% NaCl to 6.9  $\mu$ M and used for tail-vein injection. Peptide concentrations were confirmed using the Pierce Micro BCA Assay (Rockford, IL). Working solutions of PT (Sigma-Aldrich, St. Louis, MO) were diluted in 0.9% saline to  $3.0 \times 10^{-3}$   $\mu$ g/ $\mu$ l prior to use in tail vein injection. Concentrations were confirmed using the Micro BCA Assay (Pierce; Rockford, IL).

### Animal treatments

Tail vein injections of saline only (Sal), PT plus saline (PT-Sal), or PT plus A $\beta$ <sub>42</sub> peptide (PT-A $\beta$ <sub>42</sub>) were administered according to the following time intervals and concentrations. To effectively achieve a permeable BBB, PT-A $\beta$ <sub>42</sub> and PT-Sal mice were treated with PT (300 ng in 100  $\mu$ l 0.9% saline) for 3 months via tail vein injection, which has previously been shown to reliably induce increased BBB permeability in adult mice [31]. PT injections occurred on days 0, 3, 17, 33, 47, 61, and 75 of the 3-month injection period. To augment plasma levels of A $\beta$ <sub>42</sub> in mice and track its fate, soluble A $\beta$ <sub>42</sub> peptide was administered via tail vein injection (100 microliters of 6.9 micromolar in 0.9% saline) on days 7, 11, 14, 18, 21, 25, 28, 32, 35, 39, 42, 46, 49, 53, 56, 60, 63, 67, 70, 74, 77, 81, 84, 88, 91, and 95 during the same 3 month period. Given expected inherent levels of endogenous A $\beta$ <sub>42</sub> peptide present in mice which, under conditions of increased BBB permeability, can also potentially enter the brain parenchyma, and to facilitate tracking the fate of tail vein-injected, blood-borne A $\beta$ <sub>42</sub>, a subset of PT-A $\beta$ <sub>42</sub> treated mice (n = 12) were injected with FITC-labeled A $\beta$ <sub>42</sub>. In the remaining subset of PT-A $\beta$ <sub>42</sub> mice (n = 8), animals were administered unlabeled A $\beta$ <sub>42</sub> (U-A $\beta$ <sub>42</sub>) peptide to confirm observations with FITC-labeled A $\beta$ <sub>42</sub> and to address the possibility that addition of the FITC moiety to the A $\beta$ <sub>42</sub> peptide might somehow modify its behavior and/or fate in the animal. Controls for A $\beta$ <sub>42</sub> and PT were injected with similar volumes of saline (100  $\mu$ l of 0.9% saline) with or without A $\beta$  peptides following the same schedule described above. Following completion of one month of treatments, a battery of behavioral training and testing was initi-

ated and continued for around five weeks post last injection on D-95.

### Behavioral training and testing procedures

All animals were tested on five cognitive tasks (odor discrimination, passive avoidance, spatial water maze, Lashley Maze, and selective attention/disengagement) as described in detail previously (see the Supplementary Material for additional details) [75–77]. These five tasks were chosen based on their suggested sensitivity to AD-related pathologies and/or their conceptual relevance to cognitive impairments associated with AD [78, 79]. Furthermore, while AD pathology is associated with learning impairments, tests of retention are sometimes more sensitive to mild or early impairments, and several of the tests employed here are amenable to tests of long-term retention [78]. The order in which tasks were administered was designed to separate tasks based on similar motivations, processes, or motor requirements (e.g., mazes of a similar nature, activity versus passivity) to minimize any potential transfer between tasks.

For the learning tasks requiring food deprivation, *ad lib* food was removed from the animals' home cages at the end of the light cycle approximately 40 h prior to the start of training (and thus encompassing the "rest" day between successive tasks). During this deprivation period, animals were provided food in their home cages for 90 min/day during the last 2 h of the light cycle, and thus were approximately food-deprived for 16 h at the time of training or testing. To manage the large number of animals being tested, we split the animals into two batches and ran one behavioral test at a time. Each batch of animals included mice from all treatment groups. The sequential order of the behavioral tests run was as followed: Water Maze, Lashley's III Maze, Passive Avoidance, Odor Discrimination, Water Maze Retention, Lashley's III Maze Long-term, and Selective Attention.

### Odor discrimination and choice

Rodents rapidly learn to use odors to guide appetitively reinforced behaviors [75]. Here, mice learned to navigate a square field in which unique odor-marked (e.g., almond, lemon, mint) food cups were in three corners. Although food was present in each cup, it was accessible in only one cup (e.g., that marked by a mint odor). Each animal was placed in the empty corner, after which it explored the field

and eventually retrieved the single piece of available food. In subsequent trials, the location of the accessible food cup was changed, but was consistently marked by the mint odor. On successive trials, animals required less time to retrieve the food and made fewer approaches (i.e., “errors”) to food cups lacking food. In this task, poor learning performance is indicated by an increased number of errors (i.e., contacting a cup marked by an odor not associated with available food). Using this procedure, errorless performance is typically observed within 3–4 training trials.

#### *One-trial passive avoidance*

Animals learn to suppress movement to avoid contact with aversive stimuli [75]. This “passive avoidance” response is exemplified in “step-down” avoidance procedures, where commonly, an animal is placed on a platform, whereupon stepping off the platform it encounters an aversive stimulus [75]. Following only a single trial, animals are subsequently reluctant to step off a safe platform. In the present study, upon stepping off the platform, animals were exposed to a combination of bright light and a loud oscillating noise. The ratio of post-training to pre-training step-down latencies was calculated for each animal and served to index learning. It has been determined that asymptotic performance is apparent in group averages following 1–3 training trials; thus, performance after a single trial reflects (in most instances) sub-asymptotic learning and is sensitive to variations in the rate of learning between animals. Thus, higher Post/Pre-step-down latencies indicate better learning, i.e., acquired fear of leaving the safe platform.

#### *Spatial Water Maze*

For this task, animals are immersed in a round pool of opaque water from which they could escape onto a hidden (i.e., submerged) platform. The latency for animals to find the platform decreases across successive trials [80]. The performance of animals can improve across trials despite the animals beginning each trial from a new start location (i.e., efficient navigation requires the implementation of a “cognitive map”, rather than simply following a fixed route). Such a procedure mitigates against egocentric navigation (as could determine performance in the Lashley Maze) or fixed motor patterns and promotes the animals’ dependence on extra maze spatial landmarks

and is said to reflect the animal’s representation of its environment as a “cognitive map”.

During training, shorter latencies to locate the escape platform across trials is indicative of more rapid acquisition of a stable cognitive map. To estimate capacity for long-term retention in this task, animals were tested with a “probe” trial following a 30-day retention interval from completion of acquisition training. On the probe test, the escape platform was removed from the pool, and all animals were started from the same start location. A 60-s test was conducted in which the animals’ time searching in the target quadrant (that in which the escape platform was previously located) and non-target quadrants were recorded. This measure served to index long-term retention in this task, i.e., an animal with good retention should spend significantly more time in the target quadrant (previous location of the escape platform) than non-target quadrants. Conversely, an animal with poor retention would not express any preference for the target quadrant.

#### *Lashley III Maze*

Mice can learn a pattern of egocentric navigation to locate food in a maze [75]. The Lashley III Maze consists of a start box, four interconnected alleys, and a goal box containing a food reward [75]. Over trials, the latency of rats to locate the goal box decreases, as do their errors (i.e., wrong turns or retracing). Here, mice were first acclimated to the Lashley Maze, then received five training trials during which errors were recorded. Using our parameters, mice reach asymptotic levels of performance (i.e., errors decrease to a stable level) in 4–6 training trials, thus five trials is sensitive to differences in rate of learning across animals. To estimate capacity for long-term retention in this task, following a 30-day retention interval from completion of training, animals were placed in the start box and allowed to traverse the maze again for two trials. To index the long-term retention using this task the difference between the first trial after the retention interval (T7) and the average of the last two trials in the acquisition period (T5 and T6) was used for each animal.

#### *Selective attention/attentional disengagement*

In the human Stroop Interference Test Condition, subjects are instructed to name the color of the ink that is used to spell a word rather than read the word. Subjects respond more quickly and make fewer errors

when the written word and the color of ink are congruent (e.g., the word RED is spelled with red ink) relative to when the ink color and word disagree (e.g., the word RED is spelled with green ink). The increased latency and tendency to generate errors in the incongruent condition are believed to reflect a failure of selective attention, i.e., the subject is distracted from the task by the written word [81]. We have developed an analog of the Stroop Test for mice, wherein the attention directed toward an odor (or visual) cue is impaired when the animal is tested in the presence of a task-relevant visual (or odor) distractor [77, 82].

In the present task, mice were trained to perform an odor discrimination or a visual discrimination, each in a distinct context. In this manner, the context came to “instruct” the animal which discrimination to perform. After reaching asymptotic (near errorless) performance in each task, a test of selective attention was performed. For this test, the visual cues were added to the odor discrimination box. Given the previously learned instructions, the animal should ignore the visual cues and approach only the relevant odor cues. An increase in errors was deemed as a failure of the ability to selectively attend to the odor cues. After the completion of this test, the animals were subjected to a test of their capacity to disengage from the previous tendency to approach the odor cues. For this test, animals were placed in the visual discrimination box with both visual cues (the relevant targets) and odor cues (the task-relevant distractors) present. To perform effectively in the task, animals were required to inhibit their approach to recently reinforced odor cues and now attend only to visual cues to find food. Animals then alternated between boxes and were tested in this manner until they had been tested for performance in each box two times (for a total of four test trials). The number of errors accumulated over the test trials served as the index of selective attention and the animals’ ability to shift between relevant cues (i.e., to disengage from one type of cue and focus attention on the alternate type of cue). Errors were scored in the same manner described above for the Odor Discrimination task. A detailed description of this task is provided in the Supplementary Material.

#### *Tissue preparation for neuropathological studies*

Animals were euthanized at ~14.5 months of age using pentobarbital (200 mg/kg) administered intraperitoneally. Brains were removed rapidly and fixed in 4% paraformaldehyde in PBS at 4°C for 7 days. From each animal brain, tissue blocks were gen-

erated for immunohistochemistry (IHC), including the cerebral cortex (from multiple locations), hippocampus and cerebellum. Following fixation, tissue was either paraffin-embedded or frozen. Paraffin-embedded tissues were sectioned at a thickness of 5.0  $\mu$ m, and sections were placed on Superfrost® Plus glass slides (48311-703, VWR, Bridgeport, NJ) previously coated with Poly-L-Lysine (P8920, Sigma-Aldrich, St. Louis, MO). Slides were baked at ~60°C for 1 h to ensure tissue was fully adherent. Following fixation, tissue to be used for frozen sectioning was infiltrated with 10% and then 30% sucrose in PBS also containing 1.0% paraformaldehyde, pH 7.4) at 4°C under constant gentle agitation. Specimens were placed atop a solid 4.0% gelatin matrix and the resulting tissue/gelatin blocks were snap-frozen in liquid nitrogen and stored at -80°C. Cryosectioning was performed using a Leica CM1850 Cryostat (Deerfield, IL). Cryosections (12.0  $\mu$ m thick) were placed on Superfrost® Plus glass slides and stored in a dry container at 4°C until use.

#### *Brightfield immunohistochemistry*

Paraffin-embedded tissues were processed for brightfield IHC as described previously [30, 83, 84]. Briefly, after removal of paraffin with xylene and rehydration through a graded series of decreasing concentrations of ethanol, protein antigenicity was enhanced by microwaving sections in Target Buffer (Dako, Carpinteria, CA) for 2 min. Following a 30-min incubation in 0.3% H<sub>2</sub>O<sub>2</sub>, sections were treated for 30 min in normal blocking serum and then incubated with primary antibodies (anti-A $\beta$ <sub>42</sub> antibodies polyclonal, 1:50 dilution, AB5078P, Chemicon International, Temecula, CA; anti-mouse IgG, dilution 1:100, Millipore, Temecula, CA) for 1 h at room temperature. After a thorough rinse in PBS, a secondary biotin-labeled antibody was applied for 30 min at room temperature. Immunoreactions were treated with the avidin–peroxidase-labeled biotin complex (ABC, Vector Labs, Foster City, CA) and visualized with 3-3-diaminobenzidine-4 HCl (DAB)/H<sub>2</sub>O<sub>2</sub> (Biomedex, Foster City, CA). Sections were lightly counterstained with hematoxylin, dehydrated using increasing concentrations of ethanol, cleared in xylene and mounted in Permount. The specificity of immunoreactivity was confirmed by incorporating various antibody controls during each IHC run. Since the specificity of anti-A $\beta$ <sub>42</sub> antibodies are controversial, we used one of the most widely used

and tested anti-A $\beta$ <sub>42</sub> antibodies. All specimens were examined and photographed with a Nikon FXA microscope, and digital images were recorded using a Nikon DXM1200F digital camera and processed using Image Pro Plus (Phase 3 Imaging, Glen Mills, PA) imaging software.

#### *Fluorescent imaging*

A subset of frozen brain sections from mice treated with PT and FITC-labeled A $\beta$ <sub>42</sub> were washed in PBS, mounted using 4,6-diamidino-2-phenylindole, or DAPI (H-1500, Vector Laboratories, Burlingame, CA), and examined via fluorescence microscopy to assess the localization of FITC-conjugated peptides.

#### *Counting the number of IgG or A $\beta$ <sub>42</sub> positive neurons*

The number of A $\beta$ <sub>42</sub>-positive cells was determined from sections of brain tissue from four animals in each of the treatment groups. Sections of paraffin-embedded tissue were immunostained with anti-A $\beta$ <sub>42</sub> antibodies under identical conditions. Five random images at 20X magnification from each animals' cortical region were recorded under identical illumination, magnification and camera settings using a Nikon FXA microscope equipped with a Nikon CCD camera. Similarly, A $\beta$ <sub>42</sub>-positive cells were visualized in the five random images at 20X magnification of the frozen brain cortical region using fluorescence settings of Nikon FXA microscope and Nikon Immunofluorescence camera. The total number of A $\beta$ <sub>42</sub>-positive cells in each 20X viewing field was counted. Various statistical tools were used to test the significance of differences among the different treatment groups.

#### *Statistical analyses*

After data collection, descriptive statistics for each group was examined along with the normality of the distribution. Multiple tests were used to ensure that the data followed a normal distribution, in which case an ANOVA analysis was carried out. A mixed effects analysis was preferred when there were missing data points in animal behavioral studies. If the distribution pattern of the acquired data were not normal, unpaired, non-parametric Mann-Whitney t-tests were carried out. Analyses were carried out using SPSS (v28) and GraphPad Prism (v10) while GraphPad Prism (v10) was used to generate graphs.

## **RESULTS**

Overall, on several cognitive tasks and acquisition tests, mice treated with PT plus A $\beta$ <sub>42</sub> (PT-A $\beta$ <sub>42</sub>) showed deficits compared to mice treated with PT plus saline (in place of A $\beta$ <sub>42</sub>) (PT-Sal) or saline only (Sal). By contrast, in most tests, PT-Sal mice generally did not exhibit decrements in performance compared to Sal mice. A similar pattern was observed in tests of long-term retention, where PT-A $\beta$ <sub>42</sub> mice demonstrated a marked inability to recall trained activities relative to PT-Sal and Sal mice. Results from specific tests are described below.

#### *Odor discrimination*

No significant difference in the number of errors was observed between groups in Trial 1 (before learning could have occurred; Fig. 1A). However, closer inspection of the acquisition curves suggests that the rate of acquisition was slower in PT-A $\beta$ <sub>42</sub> mice relative to the other groups, an effect that became increasingly apparent as trials progressed. This pattern was reflected in a significantly greater number of errors ( $p < 0.01$ ) in the final two trials (Trials 4 and 5) for PT-Sal and Sal mice. These observations suggest a specific deficit in the rate of acquisition in the PT-A $\beta$ <sub>42</sub> group.

#### *Passive avoidance: post/pre-latency(s)*

PT-A $\beta$ <sub>42</sub> mice exhibited inferior performance on the passive avoidance task, but this difference did not achieve statistical significance in the overall ANOVA (Fig. 1B). However, comparisons between the PT-A $\beta$ <sub>42</sub> and Sal groups or the PT-A $\beta$ <sub>42</sub> and PT-Sal groups indicated that the performance of the PT-A $\beta$ <sub>42</sub>-treated group was significantly worse than in animals treated with PT-Sal or Sal as these comparisons reached statistical significance ( $p < 0.01$ ) (Fig. 1B). On the contrary, paired comparison between mice treated with PT-Sal and Sal were not statistically different from each other (Fig. 1B).

#### *Spatial Water Maze*

We investigated the animals' ability to learn a task (spatial navigation, Fig. 2A) and retain over a long retention interval (Fig. 2B) the learned response for all treatment groups. All groups were found to exhibit equivalent performance in their ability to learn the task across trials, i.e., the groups did not differ in their

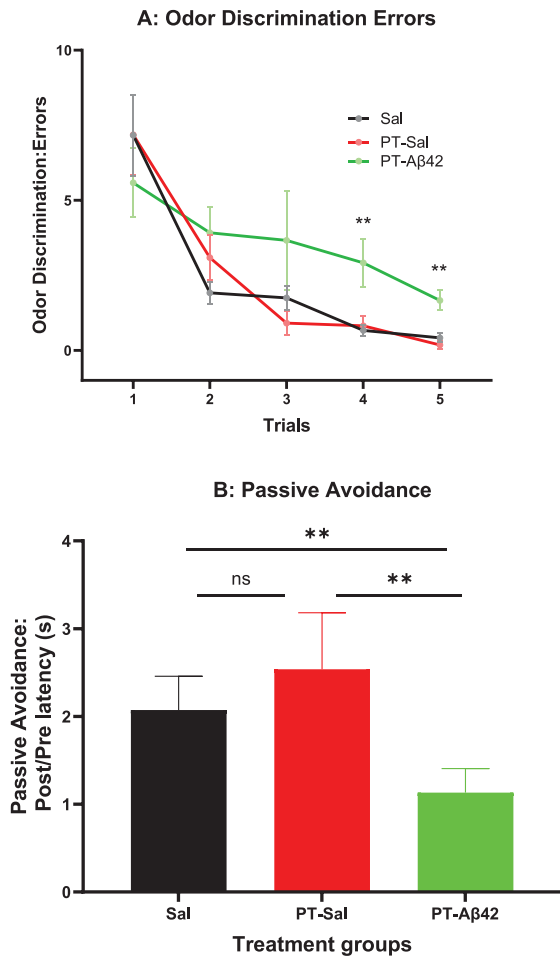


Fig. 1. Mice treated with PT-A $\beta$ <sub>42</sub> (PT-A $\beta$ <sub>42</sub>) showed deficits compared to PT-Sal and Sal-only mice. A) Odor Discrimination. Animals were trained to locate food in randomly assorted locations by using an odor cue. Mean errors to locate the target food cup for animals in each treatment group are shown. Brackets indicate standard error. Using a mixed effects analysis, we did not find any significant difference between the treatment groups across trials 1 through 3; however, when trials 4 and 5 were compared, a statistically significant difference ( $p < 0.01$ ) was observed in the PT-A $\beta$ <sub>42</sub>-treated mice compared to the other groups. B) Passive Avoidance: Post/Pre-Latency(s). Upon stepping from a safe platform, animals were exposed to a bright light, loud noise, and vibration. The mean ratio of post-training to pre-training step-down latencies was calculated for each animal and served to index learning. Brackets indicate standard errors, and the values were analyzed using the Mann-Whitney test. Animals treated with PT-A $\beta$ <sub>42</sub> showed a significantly lower step-down latency compared to the Sal group (PT-Sal,  $p < 0.01$ ). Likewise, the PT-A $\beta$ <sub>42</sub> group demonstrated significantly lower step-down latency compared to PT-Sal group ( $p < 0.01$ ). The PT-Sal and Sal-only groups failed to demonstrate any significant differences.

rate of acquisition (Fig. 2A). The latency to locate a submerged platform gradually declined in later trials (Fig. 2A), suggesting that PT-A $\beta$ <sub>42</sub> mice also learned spatial navigation at a normal rate (Fig. 2A).

On mixed effect analysis, we observed statistical difference between the trials ( $p < 0.0001$ ) without any difference between three treatment groups in each trial (Fig. 2A).

Thirty days after completion of training, the same mice were tested for long-term retention of the learned response in the Spatial Water Maze. Mice treated with PT-A $\beta$ <sub>42</sub> exhibited significant impairments of long-term retention relative to the other groups. This difference reached statistical significance in the overall Brown-Forsythe ANOVA ( $p < 0.05$ ) (Fig. 2B). Paired comparison between PT-A $\beta$ <sub>42</sub>-treated mice to PT-Sal mice as well as PT-A $\beta$ <sub>42</sub>-treated mice to Sal mice demonstrated a reduced tendency in PT-A $\beta$ <sub>42</sub>-treated mice to retain the learned task (Fig. 2B). This pattern is particularly notable given the intact acquisition observed on this task in PT-A $\beta$ <sub>42</sub>-treated animals (Fig. 2A).

#### Lashley III Maze

In the Lashley III Maze, PT-A $\beta$ <sub>42</sub>-treated mice learned how to navigate the maze in a manner comparable to mice in the other groups, as overall rates of acquisition were largely similar in this task (Fig. 2C). These values did not reflect the subjects' failure to learn, as they were evident on the first trial prior to any learning having occurred. As in the Spatial Water Maze, mice were tested for long-term retention in the Lashley III Maze at a 30-day interval. In contrast to their varying pattern of performance on tasks assessing acquisition abilities, mice treated with PT-A $\beta$ <sub>42</sub> again exhibited a performance deficit compared to the other groups (Fig. 2D). This impaired retention in PT-A $\beta$ <sub>42</sub> animals reached significance relative to mice in the Sal group ( $p < 0.05$ , Fig. 2D). A similar trend of difference in this regard was noted between the PT-Sal and Sal groups ( $p = 0.0571$ , Fig. 2D). Interestingly, paired comparison between the PT-A $\beta$ <sub>42</sub>-treated and PT-Sal-treated groups failed to attain statistical significance (Fig. 2D). Most importantly, the observed decline in retention in PT-A $\beta$ <sub>42</sub> animals was especially notable in the context of the fact that animals in all groups demonstrated comparable acquisition rates during initial training on this task (Trials 1–6, Fig. 2C).

#### Selective attention

The selective attention task is a test that is distinct from the other cognitive tasks used here. It occurs after asymptotic acquisition and makes no nominal demands on learning or long-term retention. On this test, a severe deficit was expressed by PT-A $\beta$ <sub>42</sub>

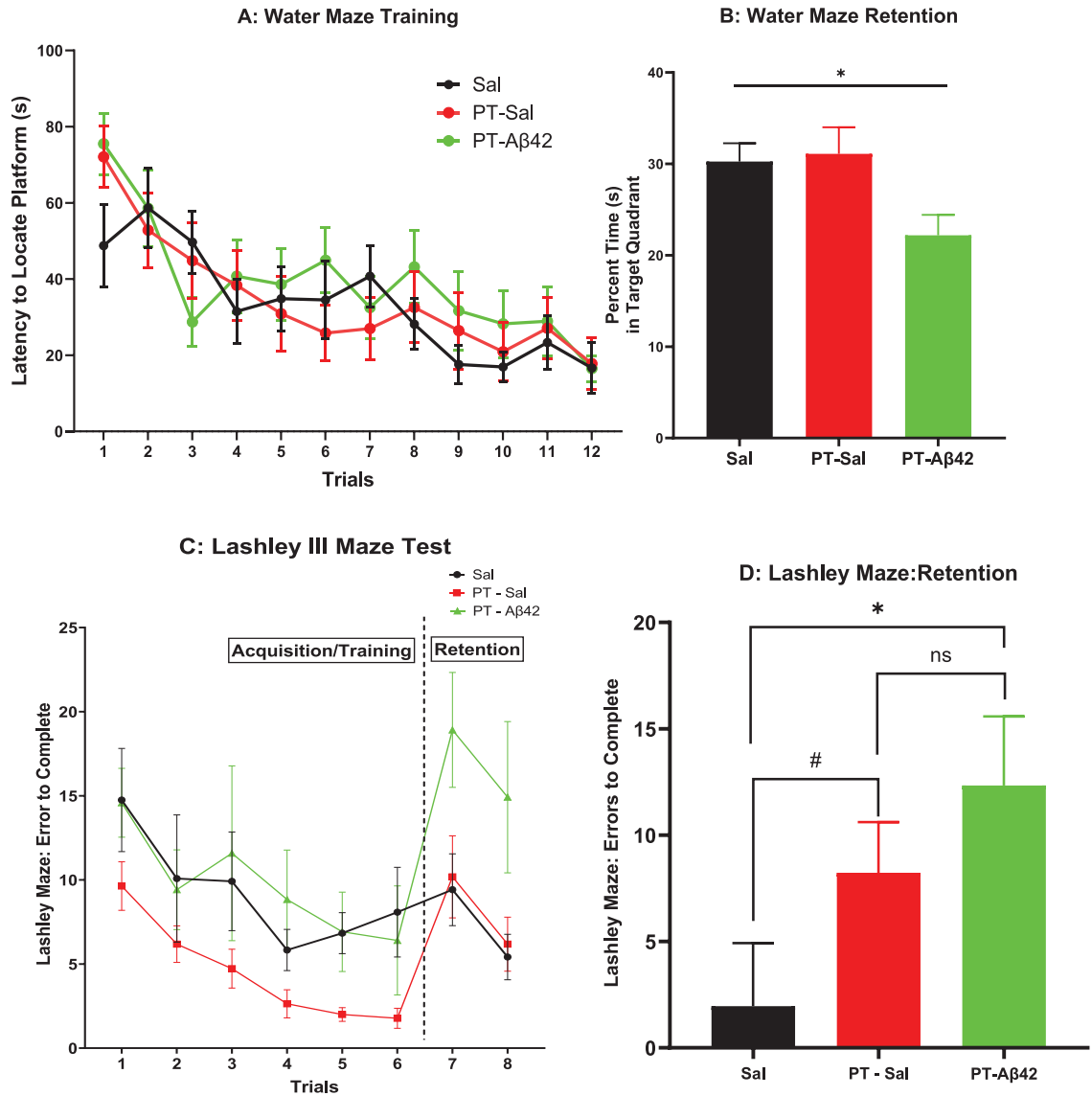


Fig. 2. A) Spatial Water Maze: Latency to Locate Platform. Animals were trained to locate a hidden platform submerged below the surface in a tank of water. The latency to locate the hidden platform was recorded across each of 12 training trials for animals in each treatment group. Brackets indicate standard error. The mice in all treatment groups demonstrated steady progress in locating submerged platform as revealed by the declined period from first to twelfth trial. Mice in all treatment groups also demonstrated comparable abilities to learn a task. B) Spatial Water Maze Retention: Percent Time(s) in Target Quadrant. Following a 30-day retention interval, animals were administered a 60-s “probe” trial in which the escape platform was removed from the maze and the percentage of time spent searching in the target quadrant was recorded. Mean time in the target quadrant is depicted. Brackets indicate standard error. For comparison across the three treatment groups, we used the Brown-Forsythe ANOVA test and found significant difference ( $p < 0.05$ ) across the treatment groups. Overall, the PT-A $\beta_{42}$  group spent less time in the target quadrant compared to both PT-Sal and Sal groups. C) Lashley Maze: Errors to Complete: Long-term Retention. Mice were trained to locate food in the Lashley Maze over 6 trials (T1–T6) and re-tested on 2 trials (T7–T8) following a 30-day retention interval. Mean errors to reach the goal box across trials are depicted for each treatment group. Brackets indicate standard error. As the training progressed, T1–T6, the number of errors was consistently reduced for mice treated with PT-Sal and Sal. Sal and PT-A $\beta_{42}$  groups demonstrated inconsistent results as their number of errors fluctuated considerably. At T7, PT-A $\beta_{42}$  mice demonstrated a significant increase in errors compared to both PT-Sal and Sal groups. The number of errors made by mice from the PT-A $\beta_{42}$  group at T7 was higher than during T1. The number of errors made by mice in the PT-Sal and Sal groups at T7 was similar and lower than T1. D) A measure of retention was computed for each animal by obtaining a difference score between the errors committed on the first post-time lapse trial (i.e., T7) and the average of the last two acquisition trials (T5–6). Brackets indicate standard error. A comparison of the errors between the Sal and PT-A $\beta_{42}$  groups attained statistical significance ( $*p = 0.0409$ ). Interestingly, between the PT-A $\beta_{42}$  and PT-Sal groups, the PT-A $\beta_{42}$  group demonstrated more errors and the numbers approached a similar trend ( $\#p = 0.0571$ ).

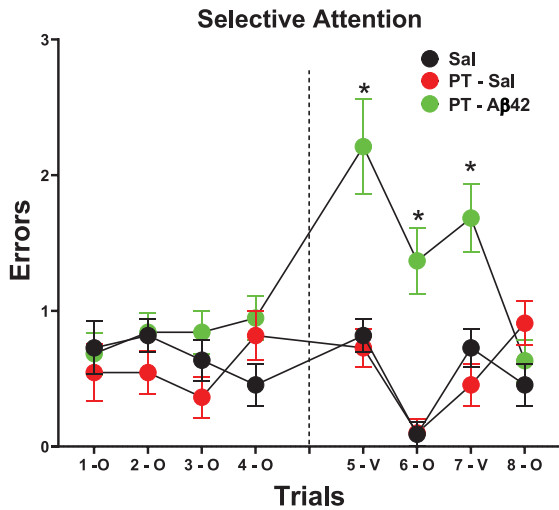


Fig. 3. **Selective Attention/Disengagement is reduced in mice treated with PT-A $\beta$ <sub>42</sub>.** Animals were trained on both odor and visual discriminations, each in a distinct context. On Trials 1- to 4, mice were tested on odor discrimination with visual discrimination cues present as distractors. All groups performed similarly on these tests. On Trials 5-8, mice were tested either on the visual discrimination with odor distractor cues present (Trials 5-V & 7-V), or on the odor discrimination with visual distractor cues present (Trials 6 & 8). PT-A $\beta$ <sub>42</sub> mice demonstrated increased errors and performed poorly relative to the PT-Sal and Sal groups. Significant differences between PT-A $\beta$ <sub>42</sub> and the other two groups are noted. These results indicated that PT-A $\beta$ <sub>42</sub> mice could not disengage from a previously reinforced cue, indicative of a failure of selective attention ( $*p < 0.05$ ).

mice relative to all other groups as determined by a trials  $\times$  Group interaction ( $p < 0.001$ , Fig. 3). This deficiency appeared to be related to an interference effect that likely accumulated across successive trials given its specific emergence on later trials when the odor cue served as the task-relevant distractor (after previously serving as the target cue; Fig. 1A). This was evidenced by significant increases in errors relative to each other group on trials 5-7, as determined by planned comparisons ( $p < 0.05$ , Fig. 3). This pattern of results suggests that PT-A $\beta$ <sub>42</sub> mice were cognitively “rigid” and could not adapt to the

changing conditions required for effective directed attention (i.e., when odor cues changed from target to distractor).

*Repetitive Pertussis toxin (PT) treatments facilitate chronic compromise of BBB integrity and leak of plasma components, including IgG antibodies, into the cerebral cortex*

To chronically increase BBB permeability in mice, PT was repeatedly injected (seven times over three months) into the tail vein as described previously [31]. Leak of IgG from the brain vasculature was used as a marker of PT-induced BBB breach in the cerebral cortex and hippocampus (Fig. 4A-D). Such leaks were observed in all PT-treated mice. Interestingly, IgG leaks did not occur uniformly along the length of brain blood vessels, but rather were variable in location and extent, and were not limited to blood vessels of a single hierarchical type. Leaks ranged from small focal plumes of material emerging from a single site (Fig. 4A, B) to more extensive leaks occurring along a greater length of the vessel and its tributaries. In general, larger vessels (especially arterioles) displayed more extensive perivascular leak clouds than smaller vessels. Areas lacking discernible leaks often exhibited a sharp interface between IgG-positive and -negative regions (Fig. 4C, D). By contrast, IgG was mostly confined to the brain vasculature in Sal mice (Fig. 4E). Thus, repetitive PT treatments facilitate chronic compromise of BBB integrity and leak of plasma components, including IgG antibodies, into the cerebral cortex.

*Chronically increased BBB permeability allows IgG antibodies to enter the brain parenchyma and bind selectively to neurons, especially pyramidal cells in the cerebral cortex*

IgG entering the brain interstitial space was found to bind preferentially to certain neuronal subtypes,

Fig. 4. **PT induces leak of plasma components and selective binding of IgG to local neurons.** A-D) Histological sections from the mouse cerebral cortex (Ctx) showing the effects of long-term PT treatment on BBB permeability. BBB leak was revealed as increased IgG immunoreactivity either widespread throughout the parenchyma or as more focused perivascular leak clouds (enclosed by dashed circles), with sharp interfaces (C, D) of IgG immunoreactivity often observed. IgG-immunopositive neurons were present within or in the vicinity of leak clouds (A, C, D). Neurons positioned more remotely from the leak showed little or no IgG labeling (black arrowheads, A-C). D) PT-A $\beta$ <sub>42</sub> mice showed the most prominent IgG leaks and most extensive labeling of the neurons. The pyramidal neurons (PNs) outside of leak zones failed to demonstrate IgG immunoreactivity (black arrowheads). E) In the Sal-only group, IgG immunoreactivity was mostly localized within the blood vessels. F) Comparison between Sal-only and PT-Sal and Sal-only and PT-A $\beta$ <sub>42</sub> attained statistical significance (Mann-Whitney test,  $p < 0.0001$ ). Though the PT-A $\beta$ <sub>42</sub> group demonstrated a higher number of PNs demonstrating IgG immunoreactivity compared to the PT-Sal group, it failed to attain statistical significance (Mann-Whitney test). Error bars indicate standard error of the mean (SEM). BV, blood vessel; Cap, capillary; Ctx, cerebral cortex. Scale bar = 50  $\mu$ m.

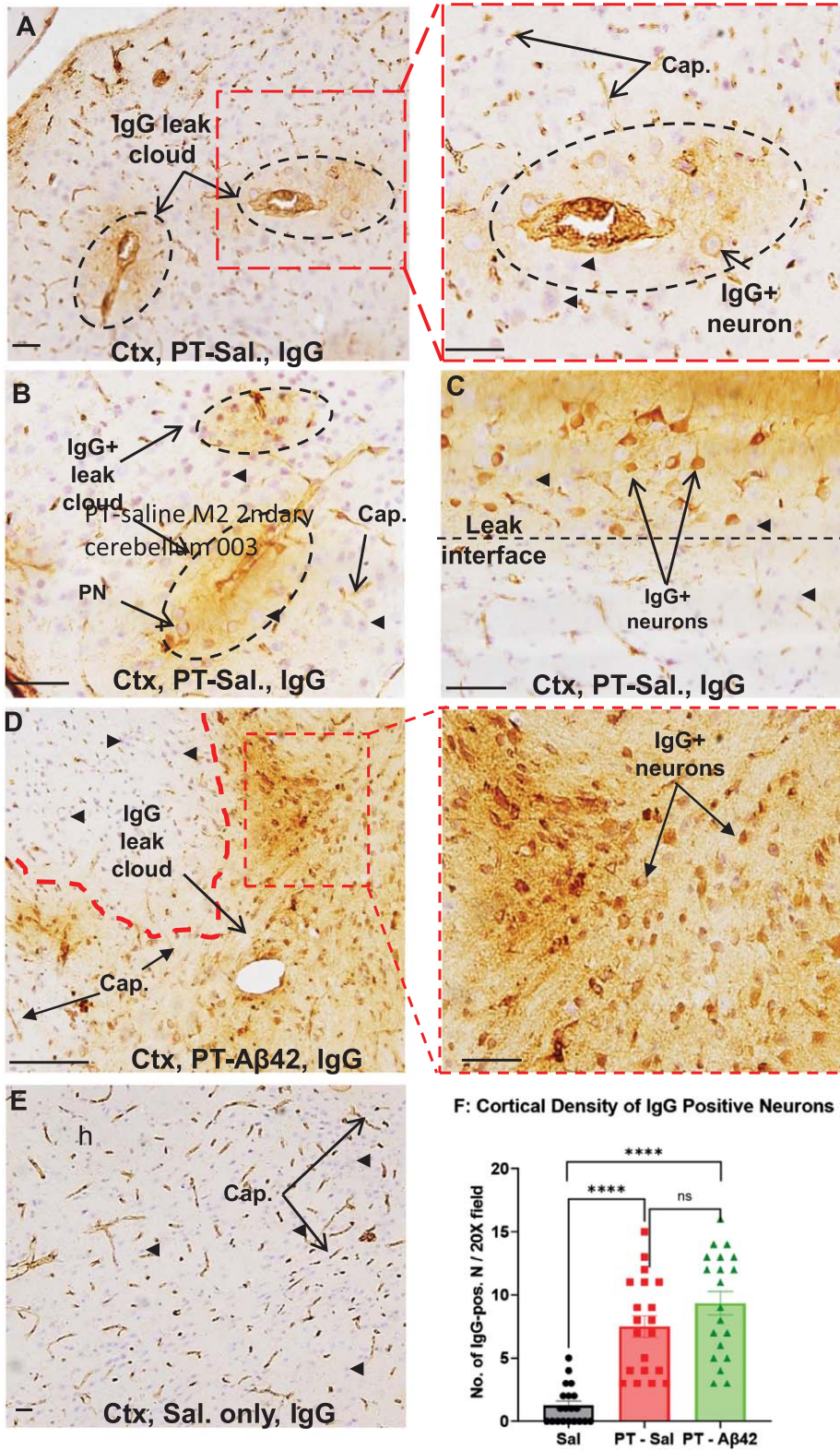


Fig. 4. (Continued)

especially pyramidal neurons positioned within or near perivascular leak clouds (Fig. 4A–D). The intensity of neuronal IgG immunoreactivity decreased rapidly with increasing distance from the vessel leak site, often forming a well-defined leak interface (Fig. 4A–D). While increased permeability of the BBB to IgG was evident in the cerebral cortex of PT-A $\beta$ <sub>42</sub> and PT-Sal mice relative to Sal controls, vascular leaks were most prevalent in the brains of PT-A $\beta$ <sub>42</sub> mice, leading to an increased cortical density of IgG-positive neurons (Fig. 4D, F). In contrast to PT-A $\beta$ <sub>42</sub> and PT-Sal animals, Sal animals exhibited a generally intact BBB within the cortex (Fig. 4E, F). We also found a significant difference in the density of IgG-positive cortical neurons across treatment groups (Fig. 4F). Paired comparison between the PT-Sal and Sal groups reached statistical significance, as did comparison of Sal mice with PT-A $\beta$ <sub>42</sub> mice ( $p < 0.0001$ ) (Fig. 4F). Although we observed a greater density of IgG-positive cortical neurons in PT-A $\beta$ <sub>42</sub> mice compared to PT-Sal mice, this difference failed to achieve statistical significance (Fig. 4F).

*Chronic BBB compromise allows bloodborne A $\beta$ <sub>42</sub> to enter the brain parenchyma and accumulate within neurons in the cerebral cortex*

The fate of exogenous A $\beta$ <sub>42</sub> in animals with and without chronic PT-induced BBB compromise was tracked over a three-month period (final age ~14.5 months) using FITC-labeled A $\beta$ <sub>42</sub> peptide administered via tail vein injection. A group of PT-injected mice also received FITC-A $\beta$ <sub>42</sub> injections throughout this period (26 times over 95 days), and the fluorescent signal was used to localize FITC-A $\beta$ <sub>42</sub> in tissue sections of the cerebral cortex (Fig. 5). In regions exhibiting vascular leak, FITC-A $\beta$ <sub>42</sub> was observed emerging from the walls of blood vessels and entering the surrounding brain interstitial space (Fig. 5A). Many (but not all) neurons within or in the vicinity of perivascular leak clouds exhibited intense FITC-A $\beta$ <sub>42</sub> fluorescence in their cytoplasm, but not in nuclei, indicating a selective affinity of exogenous FITC-A $\beta$ <sub>42</sub> for these neurons and its localization in the cytoplasmic compartment (Fig. 5A–D). As for IgG, neurons showing the greatest intensity of neuronal FITC-A $\beta$ <sub>42</sub>-positive fluorescence were those positioned closest to the source vessel (Fig. 5A, B). FITC-A $\beta$ <sub>42</sub> was also localized within numerous discrete granules in neuronal perikarya, suggesting that exogenous, cell surface-bound FITC-A $\beta$ <sub>42</sub> can be internalized and most likely

makes its way into elements of the lysosomal compartment (Fig. 5C, D). Intraneuronal deposition of FITC-labeled A $\beta$ <sub>42</sub> was clearly selective for certain types of neurons, especially pyramidal cells (Fig. 5A), with the most prominent labeling associated with larger pyramidal neurons that populate the lower layers of the cerebral cortex. Interestingly, great variations in the relative content of intracellular A $\beta$ <sub>42</sub> were observed among neurons (e.g., compare Fig. 5A–D). FITC-A $\beta$ <sub>42</sub>-positive neurons were lacking in the cerebral cortex of PT-Sal and Sal mice (Fig. 5E, F).

In PT-treated animals injected with unlabeled A $\beta$ <sub>42</sub> (U-A $\beta$ <sub>42</sub>) peptide instead of the FITC-labeled peptide, the distribution of U-A $\beta$ <sub>42</sub> in the brain following the long-term treatment course was investigated by bright field immunohistochemistry (red arrows, Fig. 6A, B). As expected, PT-U-A $\beta$ <sub>42</sub> treated mice demonstrated a U-A $\beta$ <sub>42</sub> distribution of pattern within the brain parenchyma that closely resembled that of FITC-A $\beta$ <sub>42</sub>-injected animals (red arrows, Fig. 6A, B). Controls injected with saline in place of U-A $\beta$ <sub>42</sub> showed no detectable U-A $\beta$ <sub>42</sub> in the brain parenchyma (Fig. 6C). Interestingly, PT-Sal mice (not injected with U-A $\beta$ <sub>42</sub>) also showed increased intraneuronal A $\beta$ <sub>42</sub>, although less than that of PT-U-A $\beta$ <sub>42</sub> treated mice, suggesting that endogenous mouse A $\beta$ <sub>42</sub> is also able to enter the brain parenchyma via a compromised BBB and preferentially associate and accumulate within local neurons (Fig. 6D).

*BBB compromise increases the density of A $\beta$ <sub>42</sub>-positive neurons*

We measured the density of A $\beta$ <sub>42</sub>-positive neurons (those exhibiting surface-bound and/or intracellular A $\beta$ <sub>42</sub>) in sections of the mouse cerebral cortex processed for detection of FITC-A $\beta$ <sub>42</sub> using fluorescence microscopy (Fig. 7A) or U-A $\beta$ <sub>42</sub> using Brightfield IHC and purified anti-A $\beta$ <sub>42</sub> antibodies (Fig. 7B). Fluorescence data demonstrated a significantly higher density of FITC-A $\beta$ <sub>42</sub>-positive neurons in mice injected with PT plus FITC-labeled A $\beta$ <sub>42</sub> ( $p < 0.0001$ ) compared to Sal and PT-Sal groups (Fig. 7A). Similarly, mice exposed to PT plus U-A $\beta$ <sub>42</sub> showed an increased density of U-A $\beta$ <sub>42</sub>-positive neurons within the cortex relative to PT-Sal ( $p < 0.01$ ) and Sal ( $p < 0.0001$ ) mice, (Fig. 7B). Brightfield IHC also showed a significantly higher number of A $\beta$ <sub>42</sub>-positive neurons in the PT-Sal group compared to the Sal group ( $p < 0.001$ ) (Fig. 7B).

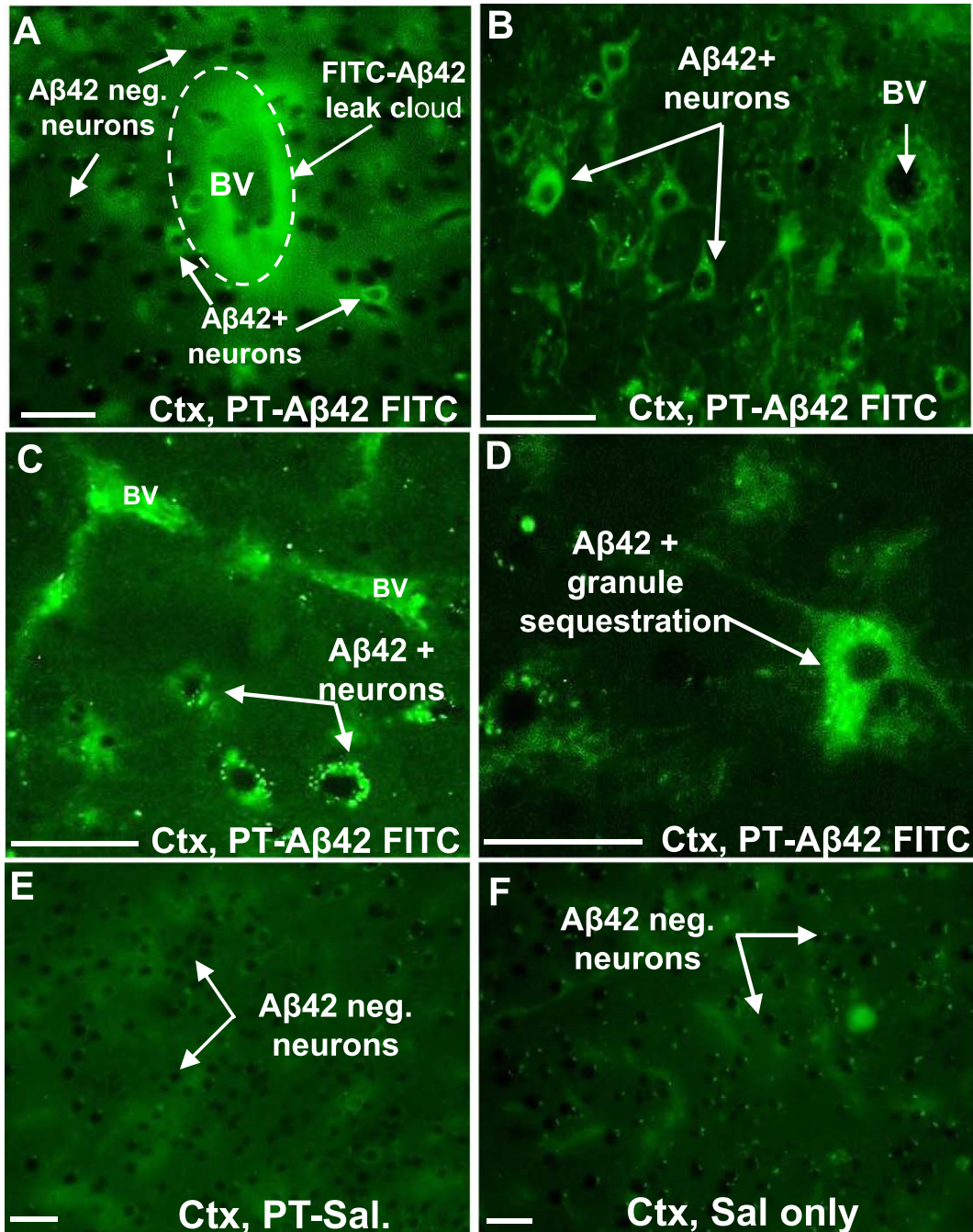
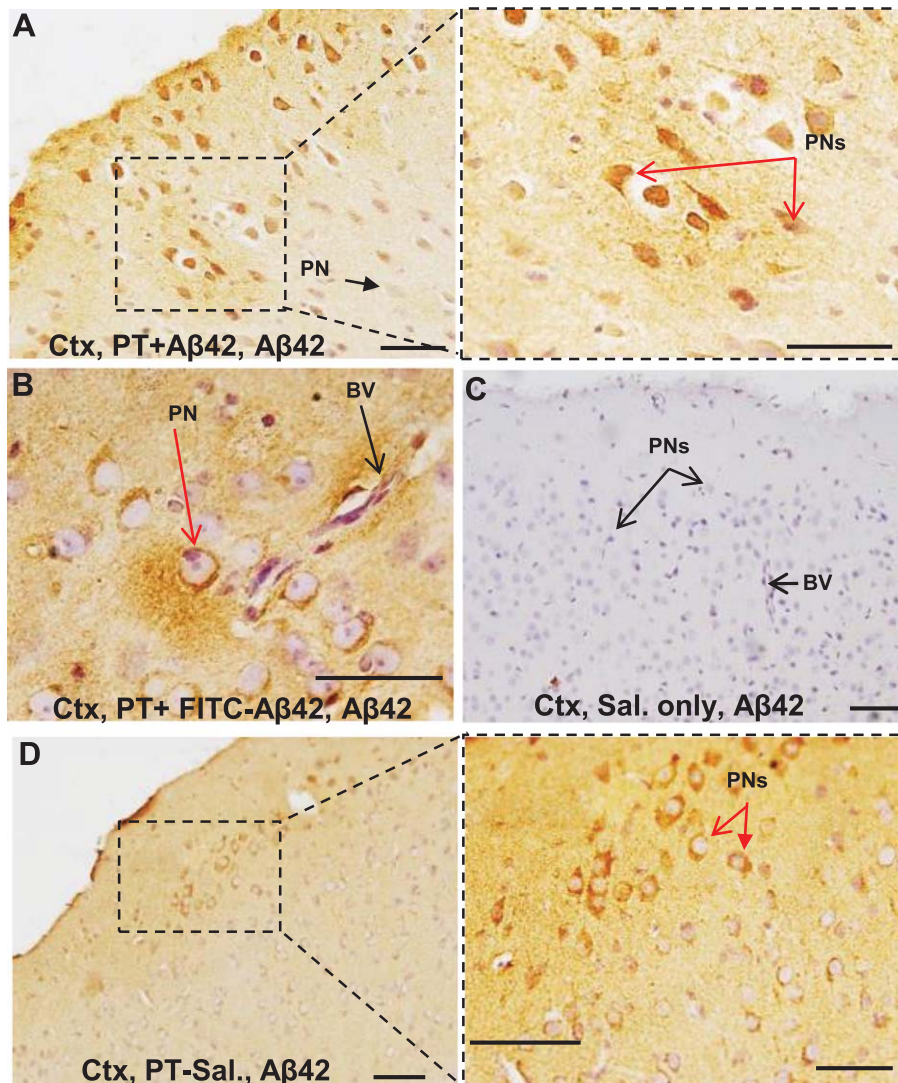


Fig. 5. FITC-labeled A $\beta$ <sub>42</sub> enters the brain parenchyma, shows selective affinity for pyramidal neurons, and is internalized within these cells. A–D) In the cerebral cortex of mice injected with PT and FITC-A $\beta$ <sub>42</sub>, FITC-A $\beta$ <sub>42</sub> leaks out from blood vessels (white dashed circle in A) and is selectively internalized in pyramidal neurons (B–D). In neurons, FITC-A $\beta$ <sub>42</sub> was localized within numerous discrete granules in the neuronal perikaryon, suggesting that cell surface-bound FITC-A $\beta$ <sub>42</sub> is internalized and accumulates within a membrane-enclosed compartment. E, F) Background fluorescence in the cerebral cortex of mice not exposed to FITC-A $\beta$ <sub>42</sub> [i.e., PT-Sal (E) and Sal-only (F)] mice. No punctate immunofluorescence like FITC-A $\beta$ <sub>42</sub> was seen in PT-Sal (E) and Sal-only (F) mice. PN, Pyramidal neurons; BV, blood vessel; Cap, capillary; PT, Pertussis toxin; Ctx, cerebral cortex. Scale bar = 50  $\mu$ m.



**Fig. 6. Cortical pyramidal neurons in mice treated with PT + unlabeled A $\beta_{42}$  (U-A $\beta_{42}$ ) peptide showed an increase in intraneuronal A $\beta_{42}$  accumulation comparable to that seen in mice treated with PT+FITC-labeled A $\beta_{42}$  (FITC-A $\beta_{42}$ ) peptide.** Bright-field immunohistochemistry with anti-A $\beta_{42}$  primary antibody was used to compare the fates of injected U-A $\beta_{42}$  and FITC-A $\beta_{42}$  in the context of PT-induced chronic BBB breakdown. A, B) Both PT + U-A $\beta_{42}$ - and PT + FITC-A $\beta_{42}$ -treated mice demonstrated increased neuronal accumulation of A $\beta_{42}$  in the cerebral cortex (Ctx), red arrows. C) No evidence of neuronal A $\beta_{42}$  deposition was observed in Sal-only mice. D) Mice in the PT-Sal group also demonstrated some intraneuronal A $\beta_{42}$ , but this was much less extensive and was often largely confined to small, isolated groups of neurons. This suggests that soluble, endogenous mouse A $\beta_{42}$  is also able to enter the brain parenchyma through a defective BBB. It is important to point out that, using the bright field microscopy, we are unable to differentiate between endogenous A $\beta_{42}$  peptides from the FITC-A $\beta_{42}$  peptide. PN, pyramidal neuron; BV, blood vessel; Cap, capillary; PT, Pertussis toxin; Sal, saline. Scale bar = 50  $\mu$ m.

#### *Accumulation of bloodborne A $\beta_{42}$ within hippocampal hilar neurons*

In PT-FITC-A $\beta_{42}$ -treated animals, the hippocampus also showed blood vessels with prominent perivascular IgG-positive leak clouds extending out into the hippocampal parenchyma (Fig. 8A, D), which were not seen in PT-Sal mice (Fig. 8B, E)

and Sal mice (Fig. 8C, F). As in the cerebral cortex, larger vessels in the hippocampus displayed the most extensive leak clouds (Fig. 8A). In mice injected with PT-FITC-A $\beta_{42}$ , the fate of FITC-A $\beta_{42}$  in the hippocampus mirrored that in the cerebral cortex. A considerable number of the large hilar neurons exhibited intense FITC-A $\beta_{42}$  fluorescence localized within discrete granules in the neuronal perikaryon,

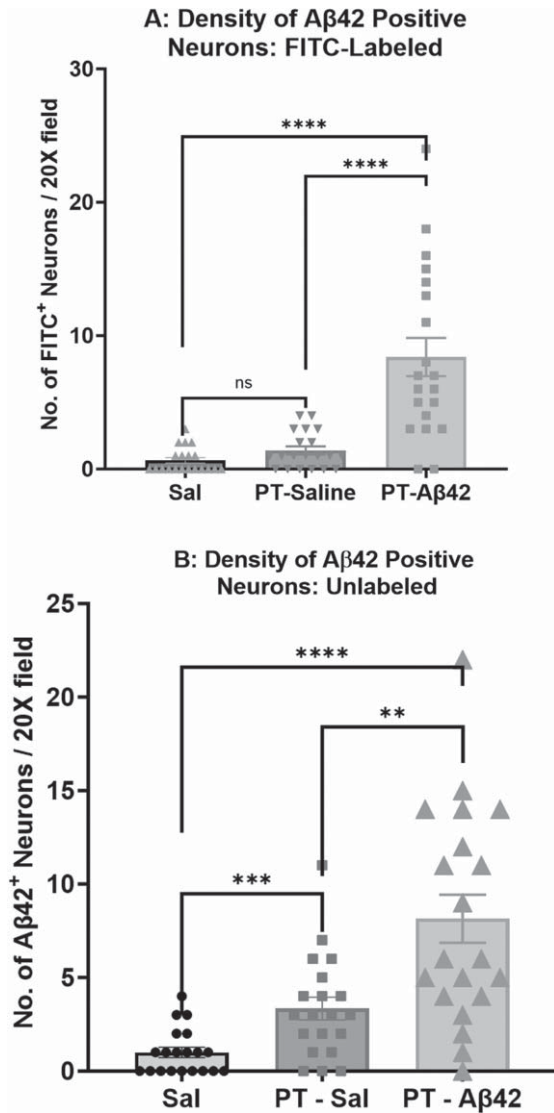


Fig. 7. The density of A $\beta$ <sub>42</sub> positive neurons in the cerebral cortex was highest in PT-A $\beta$ <sub>42</sub> mice. A) A comparison of the density of A $\beta$ <sub>42</sub>-positive neurons in mice injected with FITC-A $\beta$ <sub>42</sub> peptide was carried out by immunofluorescent microscopy. A difference in the density of A $\beta$ <sub>42</sub>-positive neurons in the cerebral cortex was detected across the three treatment groups. Comparison of the density of A $\beta$ <sub>42</sub>-positive neurons reached statistical significance (Mann-Whitney tests,  $p < 0.0001$ ) between the Sal-only and PT-FITC-A $\beta$ <sub>42</sub> groups. The difference in the density of A $\beta$ <sub>42</sub>-positive neurons also reached statistical significance (Mann-Whitney tests,  $p < 0.0001$ ) between the PT-Sal and PT-FITC-A $\beta$ <sub>42</sub> groups. B) Comparison of the density of A $\beta$ <sub>42</sub>-positive neurons reached statistical significance (Mann-Whitney tests,  $p < 0.0001$ ) between the Sal-only and PT-A $\beta$ <sub>42</sub> groups. Similarly, group comparisons between Sal and PT-Sal, and PT-Sal and PT-A $\beta$ <sub>42</sub> groups also attained statistical significance (Mann-Whitney tests,  $p < 0.001$  and  $p < 0.01$ , respectively). Error bars are standard error of the mean (SEM).

again suggesting that exogenous FITC-A $\beta$ <sub>42</sub> is selectively internalized by these neurons and most likely deposited within elements of the lysosomal compartment (Fig. 8D). No fluorescent signal similar to that from FITC-A $\beta$ <sub>42</sub> was seen in hippocampal neurons of animals PT-Sal and Sal control animals (Fig. 8E, F).

## DISCUSSION

The goal of the present study was to use an aging mouse model to investigate the effects of long-term, chronic BBB compromise on the fate of exogenous bloodborne A $\beta$ <sub>42</sub> peptide and cognitive function. To achieve this, 10-month-old mice were treated repeatedly with *Pertussis toxin* (PT) to induce a chronic increase in BBB permeability over a period of three months. During the same interval, animals were also repeatedly administered purified FITC-labeled or unlabeled A $\beta$ <sub>42</sub> via tail vein injection. Controls were similarly injected with PT plus saline or saline only. FITC-labeled A $\beta$ <sub>42</sub> was used to track the fate of bloodborne A $\beta$ <sub>42</sub> in the brain tissue. During the last month of treatment, all mice underwent extensive behavioral testing. Animals were subjected to a wide range of learning, attentional, and long-term retention tests that relied on diverse motivational and neural systems. Following completion of behavioral testing, animals were sacrificed, and the brains removed and evaluated to determine the distribution of tail vein injected A $\beta$ <sub>42</sub> peptide (FITC-labeled and unlabeled) and bloodborne IgG, both of which are normally blocked from entry into the brain in animals with a functionally intact BBB.

This study had four main findings. First, repetitive PT treatments induced a chronic increase in BBB permeability, leading to an influx of plasma components into the brain parenchyma, including IgG antibodies and FITC-labeled and unlabeled A $\beta$ <sub>42</sub> peptide. BBB leaks were evident as IgG- and A $\beta$ <sub>42</sub>-positive perivascular leak clouds in PT-treated mice and were most prominent in mice treated with PT plus A $\beta$ <sub>42</sub>. Second, after entering the brain parenchyma, both IgG and A $\beta$ <sub>42</sub> preferentially associated with certain types of neurons, mostly pyramidal neurons in the cerebral cortex and the large hilar neurons in the hippocampus. In these neurons, internalized FITC-labeled A $\beta$ <sub>42</sub> was most often localized within discrete cytoplasmic granules, presumably structures associated with the neuronal lysosomal compartment. We also found that endogenous A $\beta$ <sub>42</sub> was detectable in neurons in PT-treated mice (PT-Saline Control), but

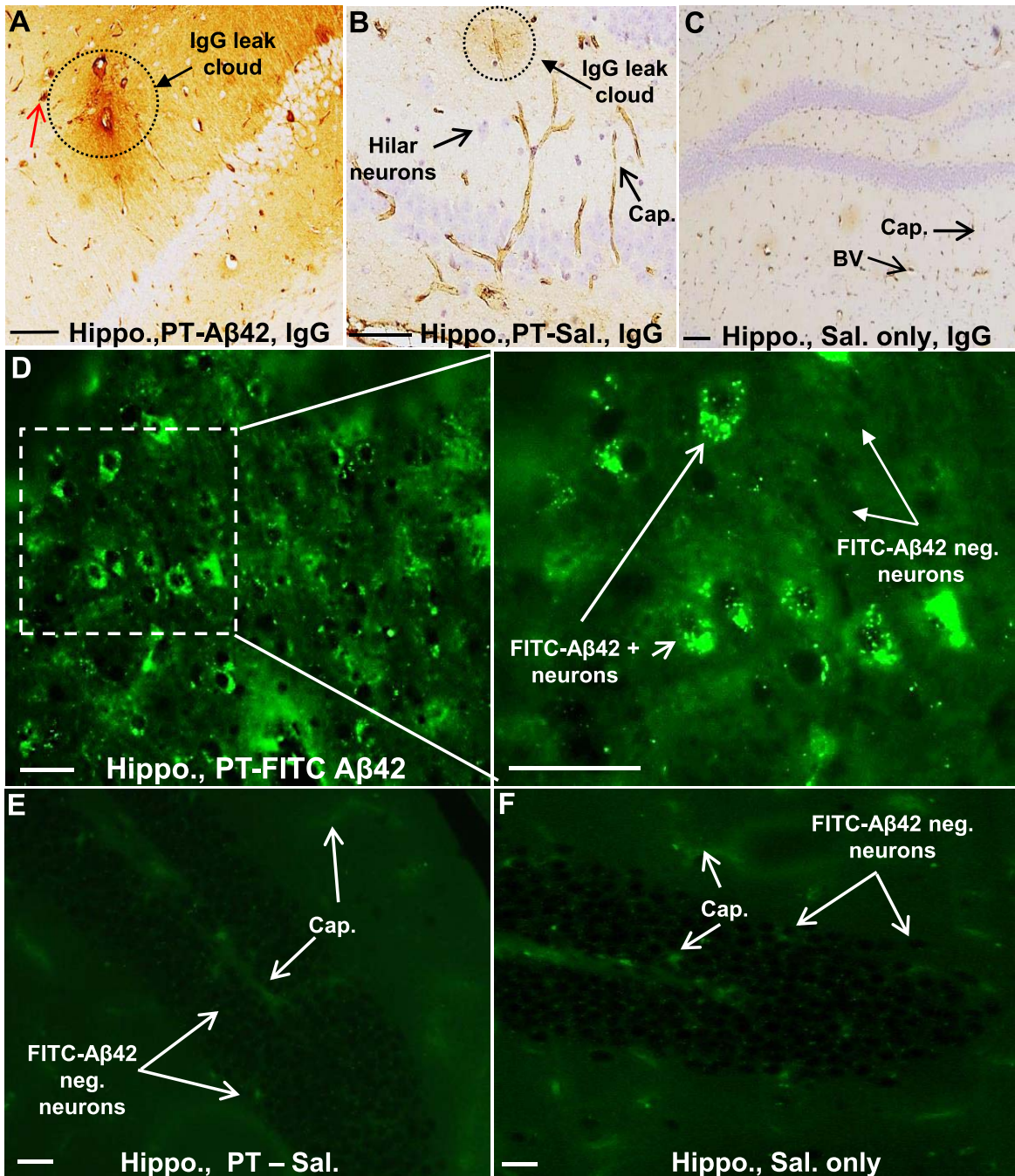


**Fig. 8. The hippocampal region of PT-A $\beta_{42}$  mice also showed increased BBB breakdown and intraneuronal accumulation of FITC-A $\beta_{42}$ .** A–C) Representative images from paraffin-embedded sections through the hippocampal region of PT-A $\beta_{42}$  mice showing extensive BBB leak of IgG compared to PT-only and Sal-only groups. D) Representative images from PT-FITC-A $\beta_{42}$ -treated mice demonstrating intraneuronal accumulation of FITC-A $\beta_{42}$  in hippocampal hilar neurons. E, F) The hippocampal region of the PT-Sal and Sal-only mice lacked FITC-positive fluorescence. Hippo, hippocampus; BV, blood vessel; Cap, capillary. Scale bar = 50  $\mu$ m.

not in mice injected with saline-only (Saline-Saline Control), suggesting that disruption of the BBB in mice is required for entry of bloodborne A $\beta_{42}$  into

brain. Third, chronic BBB compromise increased the density of A $\beta_{42}$ -positive neurons and thus total brain A $\beta_{42}$  load in animals injected with A $\beta_{42}$  via the tail

vein. Cells containing the greatest amounts of A $\beta$ <sub>42</sub> were positioned either within or in the vicinity of the leak, but no A $\beta$ <sub>42</sub>-immunopositive amyloid plaques were found in any treatment group. Fourth, with respect to cognitive functioning, animals with chronic BBB compromise and injected A $\beta$ <sub>42</sub> displayed a pattern of variable disruption of the acquisition of learned behaviors, a more consistent and preferential deficit in the capacity for long-term retention, and increased susceptibility to interference in selective attention. Taken together, these results indicate that chronic disruption of the BBB and the resulting influx of exogenous A $\beta$ <sub>42</sub> and neuron-binding IgG antibodies (autoantibodies) from the blood into the brain in mice can mimic pathological events associated with early AD-related pathology in humans as well as cause comparable early changes in behavior and cognition. In addition, our data supports the notion that blood is a likely source of exogenous A $\beta$ <sub>42</sub> peptide that eventually deposits in the brains of people afflicted with AD, with autoantibody-induced endocytosis as a route of A $\beta$ <sub>42</sub> entry into neurons.

#### *BBB compromise and AD*

Results of the present study are in accord with previous work suggesting that cerebrovascular changes are key contributors to early AD pathogenesis and subsequent disease progression [31, 54, 57, 60–62, 85–93]. Studies on humans and animal models have suggested that long-term, functional compromise of the BBB may contribute to initiation and/or progression of AD pathology, although the exact nature of its contribution is yet to be defined [30, 31, 54, 57, 60–62, 85–93]. Despite this, it is reasonable to expect that long-term increase in BBB permeability result in a chronic, gradually escalating disruption of brain homeostasis due to the influx of plasma components, including immunoglobulins (Igs) and A $\beta$  peptides, into the brain [30, 31, 92]. For obvious reasons, studies on the causal mechanisms of BBB compromise and long-term consequences in humans have been limited, necessitating the use of animal models. A missing feature that weakens the utility of mouse models for studies on the potential role of BBB compromise in AD pathogenesis is that, unlike in humans, mice lack comparable aging-associated changes in the structural/functional integrity of brain blood vessels, including those thought to lead to chronically increased BBB permeability in humans, and apparently do not live long enough to allow the full extent of AD-related pathological changes to evolve. In

a previous study, we examined the fate of FITC-labeled A $\beta$ <sub>42</sub> that was introduced into mice via a single bolus tail vein injection, with the BBB rendered permeable by a single treatment with PT [31]. This study showed that FITC-A $\beta$ <sub>42</sub> readily penetrated the BBB and was localized in neurons. To test the requirement for disruption of the BBB to allow the influx of bloodborne FITC-A $\beta$ <sub>42</sub> into the brain tissue, mice were subjected to saline injections in place of PT prior to administration of FITC-A $\beta$ <sub>42</sub> by tail vein injection. Results showed that FITC-A $\beta$ <sub>42</sub> was detected in the brain but was confined to the lumen of blood vessels, and neurons throughout the brain were devoid of FITC-A $\beta$ <sub>42</sub> [31]. In the present study, we induced a chronic, increase in BBB permeability in mice via repetitive PT injections over a period of three-months, an approach confirmed to be successful by demonstrating a resulting influx of bloodborne IgG and FITC-labeled and unlabeled A $\beta$ <sub>42</sub> into the brain parenchyma. Although PT has been widely used in developing various animal models with impaired BBB, details on how PT mediates the observed increase in BBB permeability remains poorly understood [94]. The observation of rather sharp interfaces between IgG- and A $\beta$ <sub>42</sub>-positive and -negative brain regions in these mice indicated that the site and extent of BBB compromise was not uniform in the cerebral cortex or hippocampus. A similar phenomenon has been reported in postmortem AD brains [30, 31], providing a plausible explanation for the often unpredictable pattern of symptoms that emerge early in the course of the disease, which later become more generalized as the disease progresses.

#### *Bloodborne IgG and A $\beta$ <sub>42</sub> preferentially associate with pyramidal neurons*

The present study shows that a chronic BBB compromise allows bloodborne IgG antibodies and FITC-labeled A $\beta$ <sub>42</sub> to gain access to neurons and glial within the brain parenchyma, suggesting that the blood can serve as a major source of the A $\beta$ <sub>42</sub> peptide that accumulates in AD brains under conditions of increased BBB permeability. Indeed, several studies have suggested that the blood can serve as a source of A $\beta$  peptides that deposit in the brain of AD patients [30, 31, 93, 95–98]. Here, we show that, after entering into the brain parenchyma, bloodborne IgG and FITC-labeled A $\beta$ <sub>42</sub> introduced via tail vein injection preferentially associate with neurons, most notably pyramidal neurons in the cerebral cor-

tex and large hilar neurons in the hippocampus, the same neurons that are IgG-immunopositive and have been shown to contain intracellular A $\beta$ <sub>42</sub> deposits in human AD brains [30, 31]. Of the three treatment groups, mice receiving PT + A $\beta$ <sub>42</sub> injections showed the highest number of cortical pyramidal neurons that were immunoreactive to IgG and A $\beta$ <sub>42</sub>. Cells with the largest deposits of A $\beta$ <sub>42</sub> were most often positioned within a perivascular leak cloud or in the vicinity of a leaky blood vessel. In these cells, exogenous FITC-labeled A $\beta$ <sub>42</sub> was primarily localized within discrete granules, presumably structures associated with the neuronal lysosomal compartment. Little or no blood-borne FITC-A $\beta$ <sub>42</sub> entered the brains of mice with an intact BBB (saline controls), as has been reported previously [31]. The above findings suggest a causal relationship between chronic BBB breakdown, the resulting influx of soluble A $\beta$ <sub>42</sub> and IgG into the brain tissue, the selective association and internalization of A $\beta$ <sub>42</sub> in neurons and the pathogenesis of AD.

Evidence from a number of studies demonstrates that a substantial amount of A $\beta$ <sub>42</sub> accumulates intracellularly in neurons of AD brains and in elderly mutant transgenic mice overexpressing AD-relevant genes [15, 25, 30–51]. Studies on AD transgenic mice have revealed that intraneuronal A $\beta$ <sub>42</sub> accumulation invariably precedes the appearance of plaques and temporally coincides with loss of synapses, the appearance of initial cognitive deficits and, in a triple transgenic mouse model characterized by overexpression of mutant tau, A $\beta$ PP, and presenilin (i.e., 3xTg-AD), the development of neurofibrillary tangles [15, 36, 99]. Collectively, this suggests that intraneuronal A $\beta$ <sub>42</sub> accumulation is an early event in a disease process that eventually leads, either directly or indirectly, to neuronal and synaptic loss, the appearance of amyloid plaques and neurofibrillary tangles and associated neurological sequelae [17, 36, 41, 91, 100–102]. Based on this, it has been proposed that the gradual deposition of A $\beta$ <sub>42</sub> within vulnerable neurons might progressively impair the ability of these cells to structurally and functionally support their extensive dendrite arbors and synapses, thus precipitating a gradual dendrite collapse that ultimately leads to deterioration of cognition and memory [30, 34]. Nevertheless, very little has been conclusively ascertained thus far concerning how and why A $\beta$ <sub>42</sub> accumulates selectively in certain types of neurons, why aging predisposes these neurons to do so, and how this accumulation might induce its potential effects on neuron structure and function.

#### *Possible relationship between the influx of brain-reactive antibodies and intraneuronal accumulation of A $\beta$ <sub>42</sub>*

The present study shows that the same neuronal subtypes in mouse brain that exhibit intracellular deposits of A $\beta$ <sub>42</sub> are also IgG-immunopositive, raising the possibility that the selective binding of IgG antibodies to the surfaces of these cells may somehow facilitate A $\beta$ <sub>42</sub> internalization and accumulation [30–32]. In a previous study, we tested the effects of human sera on the extent of neuronal IgG binding and intraneuronal deposition of soluble A $\beta$ <sub>42</sub> in adult mouse neurons in organotypic brain slice cultures [30]. This study showed that binding of human serum IgG to the surfaces of mouse neurons was accompanied by a dramatic increase the rate and extent of A $\beta$ <sub>42</sub> (both exogenous and endogenous) accumulation in neurons of the cerebral cortex and hippocampal region. Furthermore, replacement of human sera with specific antibodies targeting abundant neuronal surface proteins (e.g., the alpha7 nicotinic acetylcholine and glutamate R2 receptors) resulted in a comparable dramatic enhancement of exogenous A $\beta$ <sub>42</sub> internalization and accumulation in mouse cortical and hippocampal neurons, compared to neurons treated with A $\beta$ <sub>42</sub> alone [30, 103]. Taken together with the results of the present study, this suggests that increased BBB permeability allows bloodborne, brain-reactive IgG autoantibodies to access the brain interstitium and bind selectively to cognate targets on the surfaces of certain neuronal subtypes, which enhances intraneuronal deposition and accumulation of exogenous A $\beta$ <sub>42</sub> peptide, presumably via the natural tendency of neurons to clear surface-bound antibodies via endocytosis [19, 23, 30, 32, 103].

#### *Chronic, long-term BBB compromise and treatment with A $\beta$ <sub>42</sub> peptide caused deficits in cognitive functioning*

With respect to cognitive functioning, animals subjected to PT-induced, long-term BBB compromise and repeated injections of unlabeled or FITC-labeled A $\beta$ <sub>42</sub> displayed a pattern of variable disruption of the acquisition of learned behaviors, a more consistent and preferential deficit in the capacity for long-term retention, and an increased susceptibility to interference in selective attention. We used a battery of behavioral and cognitive tests aimed at assessing animals' learning (acquisition) and retention (long-term memory). Except for the

odor discrimination task (where significant learning deficits were observed), experimental manipulations such as the PT-induced increase in BBB permeability and injection of A $\beta$ <sub>42</sub> peptide had only a small and inconsistent effect on initial learning. However, mice in the PT-A $\beta$ <sub>42</sub> group demonstrated significant deficits in long-term retention as revealed by the water maze and Lashley Maze tests. The specificity of the latter effect was particularly salient in light of intact acquisition on these same tasks.

In a test of selective attention that made no explicit demands (at the time of testing) on either learning or long-term retention, mice in the PT-A $\beta$ <sub>42</sub> group expressed profound deficits. Selective attention evidenced a pattern of performance consistent with increased susceptibility to interference, manifested in specific impairment on later test trials, a segment most sensitive to accrual of interference. Since attentional abilities broadly influence cognitive processing [104, 105] this suggests that BBB breakdown and exogenous A $\beta$ <sub>42</sub> may influence general cognitive abilities that extend beyond the tasks reported here.

The aggregate pattern of functional repercussions of experimental manipulation of BBB integrity and plasma A $\beta$ <sub>42</sub> levels is particularly illuminating in view of implications for AD pathogenesis. Taken together, this profile is most consistent with a prodromal or emergent phase of AD [i.e., subtle cognitive impairment/mild cognitive impairment (MCI)], both with respect to absolute degree and distribution of impairment across domains of cognition or behavior. Individuals suffering from the amnesic variant of MCI, a subtype of MCI generally considered a transitional state for AD, typically display a specific profile that includes preferential deficits in long-term retention as compared to initial acquisition, coupled with variability in other domains of cognitive functioning. Behavioral disturbance is also common, including mild to moderate neuropsychiatric problems and mood changes such as anxiety, irritability, and apathy [106, 107]. Furthermore, the variable pattern of cognitive and behavioral deficits demonstrated here mirrors the unpredictable behavioral presentation and lack of consistent characterization of cognitive impairment associated with MCI. However, the most compelling parallels concern the specific profile of cognitive and behavioral impairment exhibited by animals treated with PT-A $\beta$ <sub>42</sub>, most prominently including a preferential deficit in long-term retention with respect to acquisition capacity, in addition to changes in selective attention. Remarkably, the pattern of results in the present model dovetails very

closely with the staging observed in longitudinal studies assessing the progression of pathology in the 3xTg-AD model, a model which surpasses the present model in progression of pathology [36, 106, 108]. In this case, studies have demonstrated that the emergence of a specific and preferential deficit in long-term retention (i.e., with respect to acquisition as well as other cognitive functions) coincides temporally with the initial appearance of intracellular accumulation of A $\beta$ <sub>42</sub>, and both can be traced to initial phases of pathological progression, corresponding to early disease stages (i.e., MCI).

#### *Limitations of the study*

This study has some inherent limitations. First is the usage of PT for compromising cerebrovasculature and BBB. Though used extensively for this purpose, PT is a toxin that can lead to inflammatory changes. Secondly, this model does not show AD-associated terminal pathological changes such as amyloid plaques, neurofibrillary tangles, and significant neuronal loss, all of which may require longer study intervals. Another limitation concerns the age of the mice. Given the consistent and robust link between advanced age and development of AD (i.e., in sporadic, non-hereditary variants of AD), this is a core feature of AD that is likely to be important in attempts to replicate pathology and determine causal mechanisms. While the age of the mice used in the present model is sufficiently advanced to allow activation of some AD-related pathological processes, their relative youth may have attenuated key mechanisms implicated in AD pathogenesis and thus curbed emergence of more dramatic pathology. Such flaws are endemic to all mouse models that attempt to translate from rodent to human pathology. Lastly, these animals lack the larger arteries found in humans, blood vessels that are most associated with susceptibility to BBB dysfunction and ensuing vascular leak given their increased hydrostatic pressure. Nevertheless, despite these potential critiques, this model is comparable to other animal models in the reproduction of early pathological and behavioral alterations associated with AD, with the advantage of exhibiting pathogenic mechanisms in the absence of forced expression of various AD-relevant genes and their gene products.

#### *Conclusions*

Results presented here indicate that plasma derived A $\beta$ <sub>42</sub> peptide and anti-neuronal autoantibodies can

penetrate a chronically defective BBB, bind selectively to the surfaces of certain types of neurons and accumulate within these cells in the characteristic pattern of AD. These findings demonstrate that chronic BBB compromise and the ensuing influx of exogenous A $\beta$ <sub>42</sub> and anti-neuronal autoantibodies from the blood over time can initiate or at least contribute to a cascade of neurological events and associated cognitive and behavioral changes that resemble those apparent in emerging AD. Taken in the context of research indicating widespread BBB deficiency in AD brains, these findings provide compelling evidence that the blood may serve as a chronic source of A $\beta$ <sub>42</sub> peptides as well as neuron-binding autoantibodies in AD as they gain access to the brain tissue through a compromised BBB, and that the influx of soluble, exogenous A $\beta$ <sub>42</sub> into the brain may be the origin of the intracellular A $\beta$ <sub>42</sub> that accumulates within neurons early in AD pathogenesis.

## AUTHOR CONTRIBUTIONS

Robert G Nagele (Conceptualization; Data curation; Formal analysis; Funding acquisition; Investigation; Methodology; Project administration; Resources; Software; Supervision; Writing – original draft; Writing – review & editing); Nimish K. Acharya (Formal analysis; Funding acquisition; Investigation; Methodology; Visualization; Writing – original draft; Writing – review & editing); Henya C. Grossman (Data curation); Peter M. Clifford (Data curation; Investigation; Methodology); Eli C. Levin (Data curation; Methodology); Kenneth R. Light (Data curation; Methodology); Hana Choi (Methodology); Randel L. Swanson (Formal analysis); Mary C. Kosciuk (Data curation; Methodology; Writing – review & editing); Venkat Venkataraman (Formal analysis; Investigation; Methodology); David J. Libon (Conceptualization; Writing – review & editing); Louis D. Matzel (Conceptualization; Formal analysis; Funding acquisition; Investigation; Methodology; Project administration; Writing – review & editing).

## ACKNOWLEDGMENTS

This manuscript includes a portion of the PhD thesis/dissertation work completed by Henya C Grossman (mentors, L Matzel and R Nagele) and Kenneth R Light (mentor, L Matzel), all of whom are co-authors.

The contents of this work do not represent the views of the Department of the Veterans Affairs or the US Government.

## FUNDING

This work was supported by funds from the Osteopathic Heritage Foundation Endowment Intramural Funding Program and Rowan School of Osteopathic Medicine (to NKA and RGN), National Institute of Aging (NIA48387-06 to LDM), Alzheimer's Association (to RGN) and Foundation of UMDNJ (RGN). RLS was supported, in part, by the US Department of Veterans Affairs Rehabilitation Research and Development Service under award number IK2 RX003651.

## CONFLICT OF INTEREST

RGN and DJL are Editorial Board Members of this journal but were not involved in the peer-review process of this article nor had access to any information regarding its peer-review.

The authors have no other conflict of interest to report.

## DATA AVAILABILITY

The data supporting the findings of this study are available within the article and/or its supplementary material.

## SUPPLEMENTARY MATERIAL

The supplementary material is available in the electronic version of this article: <https://dx.doi.org/10.3233/JAD-231028>.

## REFERENCES

- [1] Braak H, Braak E (1991) Neuropathological staging of Alzheimer-related changes. *Acta Neuropathol* **82**, 239-259.
- [2] Braak H, Braak E (1991) Demonstration of amyloid deposits and neurofibrillary changes in whole brain sections. *Brain Pathol* **1**, 213-216.
- [3] Blennow K, de Leon MJ, Zetterberg H (2006) Alzheimer's disease. *Lancet* **368**, 387-403.
- [4] Breijjeh Z, Karaman R (2020) Comprehensive review on Alzheimer's disease: Causes and treatment. *Molecules* **25**, 5789.
- [5] Scheltens P, Blennow K, Breteler MM, de Strooper B, Frisoni GB, Salloway S, Van der Flier WM (2016) Alzheimer's disease. *Lancet* **388**, 505-517.

- [6] (2020) 2020 Alzheimer's disease facts and figures. *Alzheimers Dement* **16**, 391-460.
- [7] Casey DA, Antimisiaris D, O'Brien J (2010) Drugs for Alzheimer's disease: Are they effective? *P T* **35**, 208-211.
- [8] Mehta D, Jackson R, Paul G, Shi J, Sabbagh M (2017) Why do trials for Alzheimer's disease drugs keep failing? A discontinued drug perspective for 2010-2015. *Expert Opin Investig Drugs* **26**, 735-739.
- [9] Becker RE, Greig NH, Giacobini E (2008) Why do so many drugs for Alzheimer's disease fail in development? Time for new methods and new practices? *J Alzheimers Dis* **15**, 303-325.
- [10] Wilson RS, Segawa E, Boyle PA, Anagnos SE, Hizez LP, Bennett DA (2012) The natural history of cognitive decline in Alzheimer's disease. *Psychol Aging* **27**, 1008-1017.
- [11] Li G, Larson EB, Shofar JB, Crane PK, Gibbons LE, McCormick W, Bowen JD, Thompson ML (2017) Cognitive trajectory changes over 20 years before dementia diagnosis: A large cohort study. *J Am Geriatr Soc* **65**, 2627-2633.
- [12] Jorm AF, Masaki KH, Petrovitch H, Ross GW, White LR (2005) Cognitive deficits 3 to 6 years before dementia onset in a population sample: The Honolulu-Asia aging study. *J Am Geriatr Soc* **53**, 452-455.
- [13] Emrani S, Lamar M, Price CC, Wasserman V, Matusz E, Au R, Swenson R, Nagele R, Heilmann KM, Libon DJ (2020) Alzheimer's/vascular spectrum dementia: Classification in addition to diagnosis. *J Alzheimers Dis* **73**, 63-71.
- [14] Morris JC, Price JL (2001) Pathologic correlates of nondemented aging, mild cognitive impairment, and early-stage Alzheimer's disease. *J Mol Neurosci* **17**, 101-118.
- [15] Oddo S, Caccamo A, Kitazawa M, Tseng BP, LaFerla FM (2003) Amyloid deposition precedes tangle formation in a triple transgenic model of Alzheimer's disease. *Neurobiol Aging* **24**, 1063-1070.
- [16] Brier MR, Gordon B, Friedrichsen K, McCarthy J, Stern A, Christensen J, Owen C, Aldea P, Su Y, Hassenstab J, Cairns NJ, Holtzman DM, Fagan AM, Morris JC, Benzinger TL, Ances BM (2016) Tau and Abeta imaging, CSF measures, and cognition in Alzheimer's disease. *Sci Transl Med* **8**, 338ra366.
- [17] Ossenkoppele R, Zwan MD, Tolboom N, van Assema DM, Adriaanse SF, Kloet RW, Boellaard R, Windhorst AD, Barkhof F, Lammertsma AA, Scheltens P, van der Flier WM, van Berckel BN (2012) Amyloid burden and metabolic function in early-onset Alzheimer's disease: Parietal lobe involvement. *Brain* **135**, 2115-2125.
- [18] Klunk WE, Engler H, Nordberg A, Wang Y, Blomqvist G, Holt DP, Bergstrom M, Savitcheva I, Huang GF, Estrada S, Ausen B, Debnath ML, Barletta J, Price JC, Sandell J, Lopresti BJ, Wall A, Koivisto P, Antoni G, Mathis CA, Langstrom B (2004) Imaging brain amyloid in Alzheimer's disease with Pittsburgh Compound-B. *Ann Neurol* **55**, 306-319.
- [19] Thinakaran G, Koo EH (2008) Amyloid precursor protein trafficking, processing, and function. *J Biol Chem* **283**, 29615-29619.
- [20] O'Brien RJ, Wong PC (2011) Amyloid precursor protein processing and Alzheimer's disease. *Annu Rev Neurosci* **34**, 185-204.
- [21] De Simone A, Naldi M, Tedesco D, Milelli A, Bartolini M, Davani L, Widera D, Dallas ML, Andrisano V (2019) Investigating *in vitro* amyloid peptide 1-42 aggregation: Impact of higher molecular weight stable adducts. *ACS Omega* **4**, 12308-12318.
- [22] Wilson CA, Doms RW, Lee VM (1999) Intracellular APP processing and A beta production in Alzheimer disease. *J Neuropathol Exp Neurol* **58**, 787-794.
- [23] Koo EH, Squazzo SL (1994) Evidence that production and release of amyloid beta-protein involves the endocytic pathway. *J Biol Chem* **269**, 17386-17389.
- [24] Verdile G, Fuller S, Atwood CS, Laws SM, Gandy SE, Martins RN (2004) The role of beta amyloid in Alzheimer's disease: Still a cause of everything or the only one who got caught? *Pharmacol Res* **50**, 397-409.
- [25] Alsunusi S, Kumosani TA, Glabe CG, Huwait EA, Moselhy SS (2022) In vitro study of the mechanism of intraneuronal beta-amyloid aggregation in Alzheimer's disease. *Arch Physiol Biochem* **128**, 732-739.
- [26] Games D, Adams D, Alessandrini R, Barbour R, Berthelette P, Blackwell C, Carr T, Clemens J, Donaldson T, Gillespie F, et al. (1995) Alzheimer-type neuropathology in transgenic mice overexpressing V717F beta-amyloid precursor protein. *Nature* **373**, 523-527.
- [27] Citron M, Westaway D, Xia W, Carlson G, Diehl T, Levesque G, Johnson-Wood K, Lee M, Seubert P, Davis A, Kholodenko D, Motter R, Sherrington R, Perry B, Yao H, Strome R, Lieberburg I, Rommens J, Kim S, Schenk D, Fraser P, St George Hyslop P, Selkoe DJ (1997) Mutant presenilins of Alzheimer's disease increase production of 42-residue amyloid beta-protein in both transfected cells and transgenic mice. *Nat Med* **3**, 67-72.
- [28] Hsiao K, Chapman P, Nilsen S, Eckman C, Harigaya Y, Younkin S, Yang F, Cole G (1996) Correlative memory deficits, Abeta elevation, and amyloid plaques in transgenic mice. *Science* **274**, 99-102.
- [29] Johnson-Wood K, Lee M, Motter R, Hu K, Gordon G, Barbour R, Khan K, Gordon M, Tan H, Games D, Lieberburg I, Schenk D, Seubert P, McConlogue L (1997) Amyloid precursor protein processing and A beta42 deposition in a transgenic mouse model of Alzheimer disease. *Proc Natl Acad Sci U S A* **94**, 1550-1555.
- [30] Nagele RG, Clifford PM, Siu G, Levin EC, Acharya NK, Han M, Kosciuk MC, Venkataraman V, Zavareh S, Zarrabi S, Kinsler K, Thaker NG, Nagele EP, Dash J, Wang HY, Levitas A (2011) Brain-reactive autoantibodies prevalent in human sera increase intraneuronal amyloid-beta(1-42) deposition. *J Alzheimers Dis* **25**, 605-622.
- [31] Clifford PM, Zarrabi S, Siu G, Kinsler KJ, Kosciuk MC, Venkataraman V, D'Andrea MR, Dinsmore S, Nagele RG (2007) Abeta peptides can enter the brain through a defective blood-brain barrier and bind selectively to neurons. *Brain Res* **1142**, 223-236.
- [32] Goldwaser EL, Acharya NK, Wu H, Godsey GA, Sarkar A, DeMarshall CA, Kosciuk MC, Nagele RG (2020) Evidence that brain-reactive autoantibodies contribute to chronic neuronal internalization of exogenous amyloid-beta(1-42) and key cell surface proteins during Alzheimer's disease pathogenesis. *J Alzheimers Dis* **74**, 345-361.
- [33] Nagele RG, D'Andrea MR, Lee H, Venkataraman V, Wang HY (2003) Astrocytes accumulate A beta 42 and give rise to astrocytic amyloid plaques in Alzheimer disease brains. *Brain Res* **971**, 197-209.
- [34] Nagele RG, D'Andrea MR, Anderson WJ, Wang HY (2002) Intracellular accumulation of beta-amyloid(1-42) in neurons is facilitated by the alpha 7 nicotinic acetylcholine receptor in Alzheimer's disease. *Neuroscience* **110**, 199-211.

- [35] D'Andrea MR, Nagele RG, Wang HY, Lee DH (2002) Consistent immunohistochemical detection of intracellular beta-amyloid42 in pyramidal neurons of Alzheimer's disease entorhinal cortex. *Neurosci Lett* **333**, 163-166.
- [36] Billings LM, Oddo S, Green KN, McGaugh JL, LaFerla FM (2005) Intraneuronal Abeta causes the onset of early Alzheimer's disease-related cognitive deficits in transgenic mice. *Neuron* **45**, 675-688.
- [37] Gomez-Ramos P, Asuncion Moran M (2007) Ultrastructural localization of intraneuronal Abeta-peptide in Alzheimer disease brains. *J Alzheimers Dis* **11**, 53-59.
- [38] Takahashi RH, Milner TA, Li F, Nam EE, Edgar MA, Yamaguchi H, Beal MF, Xu H, Greengard P, Gouras GK (2002) Intraneuronal Alzheimer beta42 accumulates in multivesicular bodies and is associated with synaptic pathology. *Am J Pathol* **161**, 1869-1879.
- [39] Gouras GK, Tsai J, Naslund J, Vincent B, Edgar M, Checler F, Greenfield JP, Haroutunian V, Buxbaum JD, Xu H, Greengard P, Relkin NR (2000) Intraneuronal Abeta42 accumulation in human brain. *Am J Pathol* **156**, 15-20.
- [40] Oakley H, Cole SL, Logan S, Maus E, Shao P, Craft J, Guillozet-Bongaarts A, Ohno M, Disterhoft J, Van Eldik L, Berry R, Vassar R (2006) Intraneuronal beta-amyloid aggregates, neurodegeneration, and neuron loss in transgenic mice with five familial Alzheimer's disease mutations: Potential factors in amyloid plaque formation. *J Neurosci* **26**, 10129-10140.
- [41] Shie FS, LeBoeuf RC, Jin LW (2003) Early intraneuronal Abeta deposition in the hippocampus of APP transgenic mice. *Neuroreport* **14**, 123-129.
- [42] Wirths O, Multhaup G, Bayer TA (2004) A modified beta-amyloid hypothesis: Intraneuronal accumulation of the beta-amyloid peptide—the first step of a fatal cascade. *J Neurochem* **91**, 513-520.
- [43] Wilson EN, Abela AR, Do Carmo S, Allard S, Marks AR, Welikovitsh LA, Ducatzenzeiler A, Chudasama Y, Cuellar AC (2017) Intraneuronal amyloid beta accumulation disrupts hippocampal CR1-dependent gene expression and cognitive function in a rat model of Alzheimer disease. *Cereb Cortex* **27**, 1501-1511.
- [44] Welikovitsh LA, Do Carmo S, Magloczky Z, Szocsics P, Loke J, Freund T, Cuellar AC (2018) Evidence of intraneuronal Abeta accumulation preceding tau pathology in the entorhinal cortex. *Acta Neuropathol* **136**, 901-917.
- [45] Kienlen-Campard P, Miolet S, Tasiaux B, Octave JN (2002) Intracellular amyloid-beta 1-42, but not extracellular soluble amyloid-beta peptides, induces neuronal apoptosis. *J Biol Chem* **277**, 15666-15670.
- [46] Baker-Nigh A, Vahedi S, Davis EG, Weintraub S, Bigio EH, Klein WL, Geula C (2015) Neuronal amyloid-beta accumulation within cholinergic basal forebrain in ageing and Alzheimer's disease. *Brain* **138**, 1722-1737.
- [47] Moon M, Hong HS, Nam DW, Baik SH, Song H, Kook SY, Kim YS, Lee J, Mook-Jung I (2012) Intracellular amyloid-beta accumulation in calcium-binding protein-deficient neurons leads to amyloid-beta plaque formation in animal model of Alzheimer's disease. *J Alzheimers Dis* **29**, 615-628.
- [48] Christensen DZ, Bayer TA, Wirths O (2010) Intracellular Ass triggers neuron loss in the cholinergic system of the APP/PS1KI mouse model of Alzheimer's disease. *Neurobiol Aging* **31**, 1153-1163.
- [49] Wirths O, Bayer TA (2012) Intraneuronal Abeta accumulation and neurodegeneration: Lessons from transgenic models. *Life Sci* **91**, 1148-1152.
- [50] Kobro-Flatmoen A, Hormann TM, Gouras G (2023) Intracellular amyloid-beta in the normal rat brain and human subjects and its relevance for Alzheimer's disease. *J Alzheimers Dis* **95**, 719-733.
- [51] LaFerla FM, Green KN, Oddo S (2007) Intracellular amyloid-beta in Alzheimer's disease. *Nat Rev Neurosci* **8**, 499-509.
- [52] Umeda T, Tomiyama T, Sakama N, Tanaka S, Lambert MP, Klein WL, Mori H (2011) Intraneuronal amyloid beta oligomers cause cell death via endoplasmic reticulum stress, endosomal/lysosomal leakage, and mitochondrial dysfunction *in vivo*. *J Neurosci Res* **89**, 1031-1042.
- [53] Bayer TA, Wirths O (2011) Intraneuronal Abeta as a trigger for neuron loss: Can this be translated into human pathology? *Biochem Soc Trans* **39**, 857-861.
- [54] Jeynes B, Provias J (2011) The case for blood-brain barrier dysfunction in the pathogenesis of Alzheimer's disease. *J Neurosci Res* **89**, 22-28.
- [55] Hay JR, Johnson VE, Young AM, Smith DH, Stewart W (2015) Blood-brain barrier disruption is an early event that may persist for many years after traumatic brain injury in humans. *J Neuropathol Exp Neurol* **74**, 1147-1157.
- [56] Goodall EF, Wang C, Simpson JE, Baker DJ, Drew DR, Heath PR, Saffrey MJ, Romero IA, Wharton SB (2018) Age-associated changes in the blood-brain barrier: Comparative studies in human and mouse. *Neuropathol Appl Neurobiol* **44**, 328-340.
- [57] Goldwaser EL, Acharya NK, Sarkar A, Godsey G, Nagele RG (2016) Breakdown of the cerebrovasculature and blood-brain barrier: A mechanistic link between diabetes mellitus and Alzheimer's disease. *J Alzheimers Dis* **54**, 445-456.
- [58] Erdo F, Denes L, de Lange E (2017) Age-associated physiological and pathological changes at the blood-brain barrier: A review. *J Cereb Blood Flow Metab* **37**, 4-24.
- [59] Alluri H, Shaji CA, Davis ML, Tharakan B (2018) A mouse controlled cortical impact model of traumatic brain injury for studying blood-brain barrier dysfunctions. *Methods Mol Biol* **1717**, 37-52.
- [60] Zlokovic BV (2008) The blood-brain barrier in health and chronic neurodegenerative disorders. *Neuron* **57**, 178-201.
- [61] Sweeney MD, Montagne A, Sagare AP, Nation DA, Schneider LS, Chui HC, Harrington MG, Pa J, Law M, Wang DJJ, Jacobs RE, Doubal FN, Ramirez J, Black SE, Nedergaard M, Benveniste H, Dichgans M, Iadecola C, Love S, Bath PM, Markus HS, Salman RA, Allan SM, Quinn TJ, Kalaria RN, Werring DJ, Carare RO, Touyz RM, Williams SCR, Moskowitz MA, Katusic ZS, Lutz SE, Lazarov O, Minshall RD, Rehman J, Davis TP, Wellington CL, Gonzalez HM, Yuan C, Lockhart SN, Hughes TM, Chen CLH, Sachdev P, O'Brien JT, Skoog I, Pantoni L, Gustafson DR, Biessels GJ, Wallin A, Smith EE, Mok V, Wong A, Passmore P, Barkof F, Muller M, Breteler MMB, Roman GC, Hamel E, Seshadri S, Gottesman RF, van Buchem MA, Arvanitakis Z, Schneider JA, Drewes LR, Hachinski V, Finch CE, Toga AW, Wardlaw JM, Zlokovic BV (2019) Vascular dysfunction—The disregarded partner of Alzheimer's disease. *Alzheimers Dement* **15**, 158-167.
- [62] Montagne A, Barnes SR, Sweeney MD, Halliday MR, Sagare AP, Zhao Z, Toga AW, Jacobs RE, Liu CY, Amezcua L, Harrington MG, Chui HC, Law M, Zlokovic BV (2015) Blood-brain barrier breakdown in the aging human hippocampus. *Neuron* **85**, 296-302.
- [63] Kalaria RN (2016) Neuropathological diagnosis of vascular cognitive impairment and vascular dementia with

- implications for Alzheimer's disease. *Acta Neuropathol* **131**, 659-685.
- [64] Toledo JB, Arnold SE, Raible K, Brettschneider J, Xie SX, Grossman M, Monsell SE, Kukull WA, Trojanowski JQ (2013) Contribution of cerebrovascular disease in autopsy confirmed neurodegenerative disease cases in the National Alzheimer's Coordinating Centre. *Brain* **136**, 2697-2706.
- [65] Andreasen N, Blennow K (2002) Beta-amyloid (A $\beta$ ) protein in cerebrospinal fluid as a biomarker for Alzheimer's disease. *Peptides* **23**, 1205-1214.
- [66] Feinkohl I, Schipke CG, Kruppa J, Menne F, Winterer G, Pischon T, Peters O (2020) Plasma amyloid concentration in Alzheimer's disease: Performance of a high-throughput amyloid assay in distinguishing Alzheimer's disease cases from controls. *J Alzheimers Dis* **74**, 1285-1294.
- [67] Tapiola T, Alafuzoff I, Herukka SK, Parkkinen L, Hartikainen P, Soininen H, Pirttila T (2009) Cerebrospinal fluid beta-amyloid 42 and tau proteins as biomarkers of Alzheimer-type pathologic changes in the brain. *Arch Neurol* **66**, 382-389.
- [68] Tapiola T, Pirttila T, Mikkonen M, Mehta PD, Alafuzoff I, Koivisto K, Soininen H (2000) Three-year follow-up of cerebrospinal fluid tau, beta-amyloid 42 and 40 concentrations in Alzheimer's disease. *Neurosci Lett* **280**, 119-122.
- [69] Lewczuk P, Esselmann H, Otto M, Maler JM, Henkel AW, Henkel MK, Eikenberg O, Antz C, Krause WR, Reulbach U, Kornhuber J, Wiltfang J (2004) Neurochemical diagnosis of Alzheimer's dementia by CSF A $\beta$ <sub>42</sub>/A $\beta$ <sub>40</sub> ratio and total tau. *Neurobiol Aging* **25**, 273-281.
- [70] Xu C, Zhao L, Dong C (2022) A Review of application of A $\beta$ <sub>42</sub>/A $\beta$ <sub>40</sub> ratio in diagnosis and prognosis of Alzheimer's disease. *J Alzheimers Dis* **90**, 495-512.
- [71] Levin EC, Acharya NK, Han M, Zavareh SB, Sedeyn JC, Venkataraman V, Nagele RG (2010) Brain-reactive autoantibodies are nearly ubiquitous in human sera and may be linked to pathology in the context of blood-brain barrier breakdown. *Brain Res* **1345**, 221-232.
- [72] Acharya NK, Levin EC, Clifford PM, Han M, Tourtelotte R, Chamberlain D, Pollaro M, Coretti NJ, Kosciuk MC, Nagele EP, Demarshall C, Freeman T, Shi Y, Guan C, Macphee CH, Wilensky RL, Nagele RG (2013) Diabetes and hypercholesterolemia increase blood-brain barrier permeability and brain amyloid deposition: Beneficial effects of the LpPLA2 inhibitor darapladib. *J Alzheimers Dis* **35**, 179-198.
- [73] Acharya NK, Goldwaser EL, Forsberg MM, Godsey GA, Johnson CA, Sarkar A, DeMarshall C, Kosciuk MC, Dash JM, Hale CP, Leonard DM, Appelt DM, Nagele RG (2015) Sevoflurane and Isoflurane induce structural changes in brain vascular endothelial cells and increase blood-brain barrier permeability: Possible link to postoperative delirium and cognitive decline. *Brain Res* **1620**, 29-41.
- [74] Zagorski MG, Yang J, Shao H, Ma K, Zeng H, Hong A (1999) Methodological and chemical factors affecting amyloid beta peptide amyloidogenicity. *Methods Enzymol* **309**, 189-204.
- [75] Matzel LD, Han YR, Grossman H, Karnik MS, Patel D, Scott N, Specht SM, Gandhi CC (2003) Individual differences in the expression of a "general" learning ability in mice. *J Neurosci* **23**, 6423-6433.
- [76] Matzel LD, Townsend DA, Grossman H, Han YR, Hale G, Zappulla M, Light K, Kolata S (2006) Exploration in outbred mice covaries with general learning abilities irrespective of stress reactivity, emotionality, and physical attributes. *Neurobiol Learn Mem* **86**, 228-240.
- [77] Kolata S, Light K, Grossman HC, Hale G, Matzel LD (2007) Selective attention is a primary determinant of the relationship between working memory and general learning ability in outbred mice. *Learn Mem* **14**, 22-28.
- [78] Webster SJ, Bachstetter AD, Nelson PT, Schmitt FA, Van Eldik LJ (2014) Using mice to model Alzheimer's dementia: An overview of the clinical disease and the preclinical behavioral changes in 10 mouse models. *Front Genet* **5**, 88.
- [79] Puzzo D, Lee L, Palmeri A, Calabrese G, Arancio O (2014) Behavioral assays with mouse models of Alzheimer's disease: Practical considerations and guidelines. *Biochem Pharmacol* **88**, 450-467.
- [80] Morris RGM (1981) Spatial localization does not require the presence of local cues. *Learn Motiv* **12**, 239-260.
- [81] Stroop JR (1935) Studies of interference in serial verbal reactions. *J Exp Psychol* **18**, 643-662.
- [82] Light KR, Kolata S, Wass C, Denman-Brice A, Zagalsky R, Matzel LD (2010) Working memory training promotes general cognitive abilities in genetically heterogeneous mice. *Curr Biol* **20**, 777-782.
- [83] D'Andrea MR, Nagele RG (2010) Morphologically distinct types of amyloid plaques point the way to a better understanding of Alzheimer's disease pathogenesis. *Biotech Histochem* **85**, 133-147.
- [84] Acharya NK, Nagele EP, Han M, Coretti NJ, DeMarshall C, Kosciuk MC, Boulos PA, Nagele RG (2012) Neuronal PAD4 expression and protein citrullination: Possible role in production of autoantibodies associated with neurodegenerative disease. *J Autoimmun* **38**, 369-380.
- [85] Zipser BD, Johanson CE, Gonzalez L, Berzin TM, Tavares R, Hulette CM, Vitek MP, Hovanesian V, Stopa EG (2007) Microvascular injury and blood-brain barrier leakage in Alzheimer's disease. *Neurobiol Aging* **28**, 977-986.
- [86] Yamazaki Y, Kanekiyo T (2017) Blood-brain barrier dysfunction and the pathogenesis of Alzheimer's disease. *Int J Mol Sci* **18**, 1965.
- [87] Verheggen ICM, de Jong JJA, van Boxtel MPJ, Gronenschild E, Palm WM, Postma AA, Jansen JFA, Verhey FRJ, Backes WH (2020) Increase in blood-brain barrier leakage in healthy, older adults. *Geroscience* **42**, 1183-1193.
- [88] van de Haar HJ, Burgmans S, Jansen JF, van Osch MJ, van Buchem MA, Muller M, Hofman PA, Verhey FR, Backes WH (2016) Blood-brain barrier leakage in patients with early Alzheimer disease. *Radiology* **281**, 527-535.
- [89] Sweeney MD, Zhao Z, Montagne A, Nelson AR, Zlokovic BV (2019) Blood-brain barrier: From physiology to disease and back. *Physiol Rev* **99**, 21-78.
- [90] Sweeney MD, Kisler K, Montagne A, Toga AW, Zlokovic BV (2018) The role of brain vasculature in neurodegenerative disorders. *Nat Neurosci* **21**, 1318-1331.
- [91] Nation DA, Sweeney MD, Montagne A, Sagare AP, D'Orazio LM, Pachicano M, Sepeshband F, Nelson AR, Buennagel DP, Harrington MG, Benzinger TJS, Fagan AM, Ringman JM, Schneider LS, Morris JC, Chui HC, Law M, Toga AW, Zlokovic BV (2019) Blood-brain barrier breakdown is an early biomarker of human cognitive dysfunction. *Nat Med* **25**, 270-276.
- [92] Mooradian AD (1988) Effect of aging on the blood-brain barrier. *Neurobiol Aging* **9**, 31-39.
- [93] Kalaria RN (1999) The blood-brain barrier and cerebrovascular pathology in Alzheimer's disease. *Ann N Y Acad Sci* **893**, 113-125.

- [94] Lu C, Pelech S, Zhang H, Bond J, Spach K, Noubade R, Blankenhorn EP, Teuscher C (2008) Pertussis toxin induces angiogenesis in brain microvascular endothelial cells. *J Neurosci Res* **86**, 2624-2640.
- [95] Zlokovic BV, Ghiso J, Mackic JB, McComb JG, Weiss MH, Frangione B (1993) Blood-brain barrier transport of circulating Alzheimer's amyloid beta. *Biochem Biophys Res Commun* **197**, 1034-1040.
- [96] Kandimalla KK, Curran GL, Holasek SS, Gilles EJ, Wengenack TM, Poduslo JF (2005) Pharmacokinetic analysis of the blood-brain barrier transport of 125I-amyloid beta protein 40 in wild-type and Alzheimer's disease transgenic mice (APP,PS1) and its implications for amyloid plaque formation. *J Pharmacol Exp Ther* **313**, 1370-1378.
- [97] Poduslo JF, Curran GL, Sanyal B, Selkoe DJ (1999) Receptor-mediated transport of human amyloid beta-protein 1-40 and 1-42 at the blood-brain barrier. *Neurobiol Dis* **6**, 190-199.
- [98] Deane R, Zlokovic BV (2007) Role of the blood-brain barrier in the pathogenesis of Alzheimer's disease. *Curr Alzheimer Res* **4**, 191-197.
- [99] Oddo S, Caccamo A, Tran L, Lambert MP, Glabe CG, Klein WL, LaFerla FM (2006) Temporal profile of amyloid-beta (Abeta) oligomerization in an *in vivo* model of Alzheimer disease. A link between Abeta and tau pathology. *J Biol Chem* **281**, 1599-1604.
- [100] Sosna J, Philipp S, Albay R, 3rd, Reyes-Ruiz JM, Baglietto-Vargas D, LaFerla FM, Glabe CG (2018) Early long-term administration of the CSF1R inhibitor PLX3397 ablates microglia and reduces accumulation of intraneuronal amyloid, neuritic plaque deposition and pre-fibrillar oligomers in 5XFAD mouse model of Alzheimer's disease. *Mol Neurodegener* **13**, 11.
- [101] Takahashi RH, Capetillo-Zarate E, Lin MT, Milner TA, Gouras GK (2013) Accumulation of intraneuronal beta-amyloid 42 peptides is associated with early changes in microtubule-associated protein 2 in neurites and synapses. *PLoS One* **8**, e51965.
- [102] Trojanowski JQ, Hampel H (2011) Neurodegenerative disease biomarkers: Guideposts for disease prevention through early diagnosis and intervention. *Prog Neurobiol* **95**, 491-495.
- [103] Kurup P, Zhang Y, Xu J, Venkitaramani DV, Haroutunian V, Greengard P, Nairn AC, Lombroso PJ (2010) Abeta-mediated NMDA receptor endocytosis in Alzheimer's disease involves ubiquitination of the tyrosine phosphatase STEP61. *J Neurosci* **30**, 5948-5957.
- [104] Burgoyne AP, Mashburn CA, Tsukahara JS, Engle RW (2022) Attention control and process overlap theory: Searching for cognitive processes underpinning the positive manifold. *Intelligence* **91**, 101629.
- [105] Sauce B, Wass C, Smith A, Kwan S, Matzel LD (2014) The external-internal loop of interference: Two types of attention and their influence on the learning abilities of mice. *Neurobiol Learn Mem* **116**, 181-192.
- [106] Dion C, Arias F, Amini S, Davis R, Penney D, Libon DJ, Price CC (2020) Cognitive correlates of digital clock drawing metrics in older adults with and without mild cognitive impairment. *J Alzheimers Dis* **75**, 73-83.
- [107] Hwang TJ, Masterman DL, Ortiz F, Fairbanks LA, Cummings JL (2004) Mild cognitive impairment is associated with characteristic neuropsychiatric symptoms. *Alzheimer Dis Assoc Disord* **18**, 17-21.
- [108] Golde TE, Janus C (2005) Homing in on intracellular Abeta? *Neuron* **45**, 639-642.